DR. BRIDGETT VONHOLDT (Orcid ID : 0000-0001-6908-1687)
DR. JENNIFER LEONARD (Orcid ID : 0000-0003-0291-7819)

Article type : Special Issue

Pleistocene climate fluctuations drove demographic history of African golden wolves (*Canis lupaster*)

Running title: Demographic history of African golden wolves

Carlos Sarabia[1†], Bridgett vonHoldt[2], Juan C. Larrasoaña[3], Vicente Uríos[4], Jennifer A. Leonard[1†]

[1] Conservation and Evolutionary Genetics Group, Estación Biológica de Doñana (EBD-CSIC)

[2] Faculty of Ecology and Evolutionary Biology, University of Princeton

[3] Instituto Geológico y Minero de España (IGME)

[4] Vertebrate Zoology Research Group, University of Alicante

[†] Corresponding authors: Carlos Sarabia (cdomsar@gmail.com); Jennifer A. Leonard (jleonard@ebd.csic.es)

This article has been accepted for publication and undergone full peer review but has not been through the copyediting, typesetting, pagination and proofreading process, which may lead to differences between this version and the Version of Record. Please cite this article as doi: 10.1111/MEC.15784

Pleistocene climate change impacted entire ecosystems throughout the world. In the northern hemisphere, the distribution of Arctic species expanded during glacial periods, while more temperate and mesic species contracted into climatic refugia, where isolation drove genetic divergence. Cycles of local cooling and warming in the Sahara region of northern Africa caused repeated contractions and expansions of savannah-like environments which connected mesic species isolated in refugia during interglacial times, possibly driving population expansions and contractions; divergence and geneflow in the associated fauna. Here we use whole genome sequences of African golden wolves (*Canis lupaster*), a generalist mesopredator with a wide distribution in northern Africa to estimate their demographic history and past episodes of geneflow. We detect a correlation between divergence times and cycles of increased aridity-associated Pleistocene glacial cycles. A complex demographic history with responses to local climate change in different lineages was found, including a relict lineage north of the High Atlas Mountains of Morocco that has been isolated for more than 18,000 years, possibly a distinct ecotype.

Keywords: carnivore, genomics, MiSTI, PSMC, *Canis anthus*

INTRODUCTION

Pleistocene climatic fluctuations shaped phylogeographic and demographic histories of many species in the northern hemisphere (Bolfíková et al., 2017; Feliner, 2011; Gómez & Lunt, 2007; Hewitt, 2000; Hewitt, 1999; Tison et al., 2014), which was periodically glaciated (Clark et al., 2009). The patterns left from repeated range shifts into glacial refugia and subsequent expansion across the higher latitudes has been best characterized in Europe (Hewitt, 2000; Hewitt, 1999). Species adapted to temperate climates saw a reduction in range and numbers of individuals during glacial periods in European and North American ecosystems, and benefited from milder climates during interglacials (Bolfíková et al., 2017; Dufresnes et al., 2020; Gómez & Lunt, 2007; Sommer & Nadachowski, 2006; Stöck et al., 2012). In tropical regions a combination of changes in incoming solar radiation and glacial-interglacial cycles influenced the extension and activity of the monsoon systems, and resulted in shifts between humid and arid conditions (Drake, Blench, Armitage, Bristow, & White, 2011; Ehrmann, Schmiedl, Beuscher, & Krüger, 2017; Emeis, Sakamoto, Wehausen, & Brumsack, 2000; Heinrich, 1988; Hoffmann et al., 2016; Larrasoaña, Roberts, & Rohling, 2013; Lézine, Hély, Grenier, Braconnot, & Krinner, 2011; Rohling, Mayewski, & Challenor, 2003; Smith, 2012). A pattern of expansion of savannah associated north African species was observed during humid periods (Bertola et al., 2016; Cosson et al., 2005; Dinis et al., 2019; Husemann, Schmitt, Zachos, Ulrich, & Habel, 2014; Iyengar et al., 2007; Leite et al., 2015; Lerp, Wronski, Pfenninger, & Plath, 2011). Desert adapted species show the opposite pattern of expansion during dry periods and reductions in distribution and population size in humid periods (Moutinho et al., 2020; Tamar et al., 2018).

The northern coast of north Africa is currently dominated by a temperate Mediterranean climate, which brings westerly rains that hardly penetrate 200 km away from coastal areas (Larrasoaña et al., 2013). Further south, the climate of tropical north Africa is driven by two monsoonal systems - the west and east African monsoons - that result in higher rainfall in the equatorial zone that decreases progressively towards the north. Although westerly- and monsoon-driven precipitation extend into the continental interior during extreme events, the overall scarcity of rainfall dictates the presence of the Sahara Desert, a hyperarid zone between 28-30 º N and 18 º N where semi-arid or savannah fauna live isolated in refugia around the periphery and in oases (Dinis et al., 2019; Husemann et al., 2014; Nicolas, Granjon, Duplantier, Cruaud, & Dobigny, 2009; Rato et al., 2007)(**Fig. 1**). Cyclic variations in the Earth´s orbit have driven changes in the amount of solar radiation received in the tropics, which is the engine that powers the monsoon system and has resulted in periodical expansion of savannah landscapes throughout much of the Sahara Desert since its inception about 14 million years ago (Ma) (Castañeda et al., 2009; Drake et al., 2008; Drake et al., 2011; Drake, Breeze, & Parker, 2013; DeMenocal, 2004; Ehrmann et al., 2017; Geyh & Thiedig, 2008; Larrasoaña et al., 2013; Smith, 2012; Tjallingii et al., 2008; Weldeab, Lea, Schneider, & Andersen, 2007). Such expansions, known as Green Sahara Periods (GSP), typically lasted for 3 to 6 thousand years (kyr) and occurred during bundles of high-amplitude boreal summer insolation maxima driven by maxima in the

eccentricity of the Earth's orbit. During periods of eccentricity minima, when boreal summer insolation peaks were subdued, the monsoon system was weakened and influenced by glacial-boundary conditions via changes in north Atlantic sea-surface temperatures (DeMenocal, 2004; Ehrmann et al., 2017; Tjallingii et al., 2008; Weldeab et al., 2007). Intensification of glacial cycles in the northern hemisphere after 2.7 Ma amplified the effect of glacial-boundary conditions and led to an overall shift to drier conditions over the Sahara (DeMenocal, 2004). Glacial periods occurred with a 100-kyr cyclicity after ca. 1.2 Ma (McClymont, Sosdian, Rosell-Melé, & Rosenthal, 2013) and, at least in the case of the last glacial period, were punctuated by short, colder periods (Heinrich stadials) that that lasted up to 1500 years (Heinrich, 1988; Hemming, 2004) and enhanced the dry conditions over the desert (Ehrmann et al., 2017). If animals are tightly associated with their habitat, their populations should expand and contract with their preferred habitat, so in GSPs semi-arid species should expand in population size and gene flow should increase between regions isolated during drier, glacial times (Dinis et al., 2019; Karssene, Nowak, Chammem, Cocchiararo, & Nouira, 2019; Leite et al., 2015; Lerp et al., 2011; Rato et al., 2007). Short-lived epochs of enhanced rainfall also occurred during the last glacial period along the northernmost (Drake et al., 2013; Hoffmann et al., 2016; Smith, 2012) and southernmost (Castañeda et al., 2009; Weldeab et al., 2007) fringes of the Sahara, and might have also driven changes in population size and gene flow in north African species.

The African golden wolf (*Canis lupaster*) is a recently re-discovered (Koepfli et al., 2015) wild canid species of north and east Africa. Its current distribution encompasses approximately 11 million square kilometers from Morocco to Egypt in the north and from Senegal to Kenya in the south (Kebede, Sciences, Box, & Sodo, 2017; Kingdon, 2013) (**Fig. 1**). This large distribution makes them useful for answering questions about how past climate periods could have affected mesic mammal communities in north Africa. Until recently, African golden wolves were considered the same species as the Eurasian golden jackal (*Canis aureus*), and most ecological data have been collected in Eurasia, making African golden wolves one of the least studied canid species in the world (Admasu, Thirgood, Bekele, & Laurenson, 2004; Amroun, Bensidhoum, Delattre, & Gaubert, 2014; Amroun, Giraudoux, & Delattre, 2006; McShane & Grettenberger, 1984). Their wide distribution and generalist predatory style has allowed them to adapt to a wide variety of habitats including arid or semi-arid landscapes, grasslands, savannahs, forests and high elevation areas in Morocco and Ethiopia as well as anthropized zones (Amroun, Oubellil, & Gaubert, 2014; Amroun et al., 2006; Cuzin, 2003; Kebede et al., 2017; McShane & Grettenberger, 1984).

Despite their large home ranges and ecological plasticity (Admasu et al., 2004; Amroun et al., 2014, 2006; Fuller, Biknevicius, Kat, Van Valkenburgh, & Wayne, 1989; Karssene et al., 2018; McShane & Grettenberger, 1984; Moehlman, 1986), African golden wolves have not been found in hyperarid areas (Kingdon, 2013) although they have been reported in archaeological sites in current-day desert areas that

were greener in the past (Sereno et al., 2008). This suggests that African golden wolves had a wider distribution during GSP. In addition to climate, competition between African golden wolves and bigger carnivores with overlapping distributions, such as hyenas (Kebede et al., 2017; Kingdon, 2013) and black-backed jackals (Van Valkenburgh & Wayne, 1994), could have affected their distribution. Recent genetic evidence has suggested that African golden wolves may have benefited from increases in human populations since the Neolithic, either through the introduction of caprid livestock that could have served as a food source, and/or through predator control against competing species (Eddine, Mostefai, et al., 2020). African golden wolves have been shown to scavenge around anthropized zones (Admasu et al., 2004; Amroun et al., 2014; Amroun et al., 2006; McShane & Grettenberger, 1984), but have disappeared from very intensively exploited agricultural areas (Aulagnier, 1992; Cuzin, 2003). Finally, recent evidence from whole genomes of African golden wolves (Chavez et al., 2019; Gopalakrishnan et al., 2018; Liu et al., 2018) have shown a complex genetic history with two separate populations at the extremes of their distribution and possibly events of introgression from other related canids in the past.

Here we use seven whole genome sequences from across the distribution of African golden wolves and recently developed analytical methods to evaluate population structure, deep demographic history, and past episodes of gene flow. We integrate the genomic results with past environmental variability in north Africa (Castañeda et al., 2009; Drake et al., 2008; Drake et al., 2011; Drake et al., 2013; Geyh & Thiedig, 2008; Larrasoaña et al., 2013; Tjallingii et al., 2008; Weldeab et al., 2007) in order to evaluate the role of monsoon variability and its teleconnection with glacial-interglacial climates in shaping the demography of the African golden wolf. We also compare the genomic diversity, structure, and inbreeding coefficients across the species with similar geographic distributions in two closely related canids (gray wolves, *Canis lupus;* and coyotes, *C. latrans*) with very different social systems and ecology. We find a complex demographic history with different, well defined populations that diverged thousands of generations ago coinciding with Late Pleistocene climatic fluctuations, and an isolated mountain lineage with a high degree of inbreeding whose genome-wide heterozygosity has been drastically reduced. Although the morphology and size of the African golden wolves is more similar to North American coyotes, the observed genetic population structure is more similar to what is found in gray wolves, possibly suggesting a social system and ecology more similar to the latter.

METHODS

Materials

A sample from a previous study (Urios, Donat-Torres, Monroy-Vilchis, & Idrissi, 2015) from which the mitochondrial genome has already been published (KT378605) was used to construct a shotgun library as in Camacho-Sanchez et al., (2018) and sequenced. The individual was a roadkill found at N32º33.364' W5º50.848', in Beni Mellal province, Morocco. The area is a hill slope at around 2000 m asl

elevation in the north of the High Atlas Mountains. We refer to this sample as "west Morocco" and a previously published genome (Gopalakrishnan et al., 2018) from another Moroccan individual as "east Morocco". An additional 26 genomes were obtained from the literature: six African golden wolves, seven domestic dogs, six gray wolves, two Eurasian golden jackals one Ethiopian wolf, one African hunting dog, and three coyotes (**Table S1**).

Pre-processing pipeline

Adapters were trimmed with cutadapt (Martin, 2011) and quality of the reads was evaluated with FastQC (Andrews, 2010). Reads were mapped using bwa mem v1.3 (Li & Durbin, 2010) to the reference genome CanFam3.1 (*Canis familiaris*, domestic dog) (Lindblad-Toh et al., 2005), with the Y chromosome (Oetjens, Martin, Veeramah, & Kidd, 2018). Reads were also mapped to an assembled reference genome of an African hunting dog (*Lycaon pictus*; Campana et al., 2016) to avoid bias from mapping to the dog genome, which is in the ingroup for some analyses. We sorted and filtered low quality mapped reads with samtools v1.9 (Li, 2011) and removed duplicates with GATK v3.7 (McKenna et al., 2010). All reads had a sequencing quality higher than 20 and had a complementary read in the same chromosome (**Table S1**).

Variant calling and quality filters

We filtered reads mapping to sex chromosomes and mitochondrial DNA and retained only autosomes. We filtered low quality mapped reads and called genotype likelihoods using ANGSD. Sites with depth <5X or more than twice the mean coverage depth were filtered out (Freedman et al., 2014). Genotype likelihood frequency files (.glf.gz) were used to call SNPs using the -doplink option in ANGSD and an exclusion zone of 10 kilobases (kb) upstream and downstream the genic regions was defined using a .refseq annotation file of CanFam3 from the UCSC Genome browser (Kent et al., 2002) and custom scripts (Supplementary Code File 02.b). Genotype likelihoods were computed and SNPs called for autosomes mapped against both reference genomes (CanFam3.1 and African hunting dog).

Genetic structure

A principal component analysis (PCA) was performed using genotype posterior probabilities of genotypes of the five Old World species with the ngsCovar package in ngsTools (Fumagalli, Vieira, Linderoth, & Nielsen, 2014) and Rscript v3.4.4 (The R Core Development Team, 2017). We estimated admixture proportions from genotype likelihoods using NGSadmix (Skotte & Albrechtsen, 2013), setting number of clusters (K) between 5 and 14. To ensure reproducibility of results, we ran the NGSadmix test five times and visually compared the plots.

We used .glf.gz files to call SNPs with ANGSD (-doPlink option, settings: -pvalue 1e-5, -doMaf 1, -doPost 1). Genic regions, deviations from Hardy-Weinberg (HW) equilibrium, and SNPs in linkage disequilibrium were filtered from the dataset in PLINK v1.9 (Purcell et al., 2007) (settings: --hwe 0.001, --maf 0.05, --indep-pairwise 50 5 0.5). We performed a PCA using flashPCA (Abraham & Inouye, 2014) and

estimated admixture composition using ADMIXTURE (Alexander, Novembre, & Lange, 2009) with a number of clusters (K) between 5 and 14. Visual comparisons were made of plots with genotype likelihoods and with discovered SNPs in genomes mapped against CanFam3.1 and the African hunting dog genome.

Demographic history

We down sampled .bam files of the Kenyan African golden wolf (AGW) to 7X, 9X, 11.2X, and 15X from 24X using samtools view -bs (Li, 2011) to visually estimate the best false negative rate (FNR) due to low coverage following (Hawkins et al., 2018; Kim et al., 2014; Nadachowska-Brzyska, Burri, Smeds, & Ellegren, 2016) and the different coverages of the Kenyan genome were plotted with and without FNR correction (**Fig. S1A,B**).

To avoid misinterpretations of heterozygous sites as homozygous in low coverage samples (e.g., 7X-15X) (Nadachowska-Brzyska, Burri, Smeds, & Ellegren, 2016), we repeated the process with the actual coverage and downsampled .bam files of the Kenyan African golden wolf (7X, 9X, 11.12X, 15X and 24X) to visually estimate the best false negative rate (FNR) following (Hawkins et al., 2018; Kim et al., 2014; Nadachowska-Brzyska et al., 2016). After determining the FNR, consensus sequences with genic regions were called with bcftools mpileup (settings: -C 50, d 5, -D 100). PSMC was called using 64 atomic time intervals (settings: -p "1*6+58*1") as in previous studies with AGW (Freedman et al., 2014), and initial theta per individual and coverage was corrected (Li & Durbin, 2011). A round of 50 iterations of bootstrapping per genome was applied to draw a multisample PSMC plot. A mutation rate of $4.5 * 10^{-9}$ (Koch et al., 2019) and generation time of 3 years (Chavez et al., 2019; Freedman et al., 2014; Gopalakrishnan et al., 2018; Koepfli et al., 2015; Liu et al., 2018) were used. To explore extreme mutation rates ($2.7\text{-}7.1 * 10^{-9}$ as estimated by Koch et al. 2019), we also generated PSMC plots for all AGWs except Egypt without bootstrapping with these values.

More recent demographic population history was studied with ngsPSMC (Shchur et al., 2019). We generated files for ngsPSMC in ANGSD (option: -dopsmc) filtering for a minimum depth of 5X per genome. We ran ngsPSMC for 50 iterations with the same atomic time intervals as in PSMC, using initial population sizes 10^5 years ago as observed in the PSMC plot. Calculated $\Theta\pi$ was used as theta (θ) (see Supplementary Code File 03) and we estimated genome wide rho from a recombination map for dogs (Auton et al., 2013). Mutation rate and generation time were the same as in PSMC. NgsPSMC is still under development, so bootstrapped plots could not be generated.

We considered both low- and high-latitude climate mechanisms influencing past environmental variability in the Sahara back to 1.5 million years ago (Castañeda et al., 2009; Drake et al., 2013; Ehrmann et al., 2017; Larrasoaña et al., 2013; McClymont et al., 2013; Rohling et al., 2003; Smith, 2012; Tjallingii

et al., 2008; Weldeab et al., 2007) that could have affected the demographic history of AGW. We compared the timing of these events with the PSMC and ngsPSMC maxima and minima and observed possible correlations between climatic events and increases or decreases of population. We also added the speciation event that led to African golden wolves (Chavez et al., 2019; Koepfli et al., 2015) with a confidence interval of 400 kyr.

Summary statistics

We inferred changes in Ne with thetas and neutrality tests based on likelihood-based estimation of site frequency spectrum (SFS) in ANGSD (Nielsen, Korneliussen, Albrechtsen, Li, & Wang, 2012). The reference genome of the African hunting dog (Campana et al., 2016) was used as ancestral to call unfolded SFS, assuming HW equilibrium, multisample GL estimation (-dosaf 1), and an upper depth filter of 2.5X, mean read depth per sample and per population as in **Table S1**. We calculated the genome wide heterozygosity per individual as in Gopalakrishnan et al. (2018). Different coverages of the Kenyan AGW (7X, 9X, 11.2X, 15X, 24X, as above) were used to repeat SFS calling and correct mean heterozygosity for all samples.

We used a joint SFS between pairs of populations (2DSFS) to estimate average genome wide Fst and 95% confidence intervals from a 50 kb sliding window scan. Finally, we computed a series of nucleotide diversity indexes (Tajima's D (Tajima, 1989), Fu and Li's F and D (Fu & Li, 1993), Fay's H (Zeng, Fu, Shi, & Wu, 2006), Zeng's E (Zeng et al., 2006)) and thetas (Θ_W, $\Theta\pi$, Θ_{FL}, Θ_H, Θ_L) (Durrett, 2008; Fay & Wu, 2000; Fu & Li, 1993; Tajima, 1989; Watterson, 1975; Zeng et al., 2006) using the -doThetas 1 option in ANGSD with population-based SFS as prior information (-pest), divided in 50-kb windows across the genome and excluding genic regions.

Heterozygosity

We defined four populations: afr_north (AGW from Algeria, Egypt, east Morocco, west Morocco, Senegal), afr_east (AGW from Ethiopia, Kenya), coyote (coyotes from California, Midwest and Mexico) and gwolf_me (gray wolves from S. Arabia, Iran and Syria). We calculated the inbreeding coefficient or F_i per individual based on individual genotype likelihoods using ngsF (Vieira, Fumagalli, Albrechtsen, & Nielsen, 2013), computed across 20 iterations in ngsF. Genotype-based calculation of F_i per individual was performed in PLINK with –het on a dataset of SNPs discovered using ANGSD (option -doPlink).

We used two approaches to calculate ROHs across the whole genome. The first method uses PLINK and the SNP dataset from the F_i calculation. In each population we removed SNPs in close linkage disequilibrium in 200 basepair (bp) windows with a step size of 100 bp and a R^2 of 0.9 using option –indep-pairwise 200 100 0.90 in PLINK and generated ROHs as in Sams & Boyko (2019). The second method uses the software ROHan (Renaud, Hanghøj, Korneliussen, Willerslev, & Orlando, 2019) on mapped .bam

files. We ran ROHan in windows of 500kb in .bam files of all AGW, coyotes and gray wolves of the Middle East. Expected theta in ROHs was set to $2*10^{-5}$ and default options for Illumina error rate. Plots of local heterozygosity were computed across the whole genome and a summary of ROHs was calculated. Finally, we calculated inbreeding coefficients from ROHs (F_{ROH}) as in (McQuillan et al., 2008; Sams & Boyko, 2019):

$$F_{ROH_j} = \frac{\sum_k length(ROH_k)}{L};$$

where ROH_k is the *k*th ROH in individual *j*'s genome and L is the total length of the genome.

Divergence dating

We used MiSTI (Shchur, 2019) to estimate times of divergence between local lineages represented by our seven AGW individuals. We used a list of green Sahara periods (Ehrmann et al., 2017; Larrasoaña et al., 2013) and of cold stadials (Heinrich, 1988; Hemming, 2004; Rohling et al., 2003) associated with increased aridity of the Sahara region (Ehrmann et al., 2017) to define humid (with potentially more connectivity among lineages) and dry (potential times for divergence) time segments. We used pairwise time scales generated using PSMC and 2DSFS files from previous sections. GNU Parallel (Tange, 2018) was used to model simultaneously different scenarios of divergence among lineages with different migration rates in dry periods and GSPs, permitting MiSTI to automatically optimize calculations of migration rate per time segment. We extracted a table of splitting times from MiSTI and plotted log likelihoods per proposed splitting time against time. Finally, a polynomial curve was fitted per group of data where $R^2 \geq 0.99$ to estimate the maximum point of the curve using the Newton-Raphson approach and a confidence interval of the upper 5%, 1% and 0.1% of log likelihood points. Since this is a new software, we evaluated the replicability of our results by testing divergence time estimations with different coverages of the same genomes and different combinations of pre-defined time segments. We also compared the results with an estimation of divergence time using the Cavalli-Sforza et al. (1969) equation (Supplementary Methods).

RESULTS

Although coverage was different between samples, for each sample coverage across the genome was similar when reads were mapped against the two reference genomes, CanFam3.1 and the African hunting dog. Coverage for samples mapped against CanFam3.1 ranged from 5.16X to 34.54X and from 4.58X to 32.1X when mapped to the African hunting dog reference genome (Campana et al., 2016)(**Tables S2** and **S3**). Mapping against CanFam3.1 resulted in a slightly higher mappability, higher coverage and less duplicates than against the African hunting dog genome (**Table S4**). The new sample, west Morocco, had a

total of 284,332,735 raw reads. Average mappability for this sample against CanFam3.1 and African hunting dog reference genomes was 93.99% and 91.55%, respectively. Genomewide coverage was 11.26X mapped against CanFam3.1 and 10.58X mapped against African hunting dog (**Tables S2** and **S3**).

Population structure driven by a north-south boundary

Genotype probabilities were calculated across 23 genomes of five species (7 African golden wolves (AGW), 7 dogs, 6 gray wolves, 1 Ethiopian wolf, 2 Eurasian golden jackals) with the -doGeno 32 option in ANGSD. Nearly three million (2.98M) sites were called when mapping against the CanFam3.1 genome, and 2.54M sites when mapping against the African hunting dog. Genotype likelihood-based SNP calling with ANGSD produced 689,000 (698K) sites for those genomes mapped against CanFam3.1, and 625K sites for genomes mapped against the African hunting dog. All SNPs were more than 10kb away from any genic zone and were in HW equilibrium. We identified population structure, with all wolves northwest (Senegal, east Morocco, west Morocco, Algeria) and southeast of the Sahara (Kenyan and Ethiopian) in different clusters (**Fig. S2**). The Egyptian AGW appeared at an intermediate genetic distance between the northwestern cluster and a cluster that encompassed all gray wolves and dogs, which is consistent with previously published studies that suggested it has introgressed ancestry (Gopalakrishnan et al., 2018; Liu et al., 2018). While different PCAs showed Ethiopian wolves at different positions with respect to the African golden wolves depending on the reference genome and the source data (glf.gz or SNPs), the structure of African golden wolves, dogs, and gray wolves remained consistent regardless of the reference genome used to map reads against (CanFam3.1 or African hunting dog) or what method was used to generate the PCA plots (genotype likelihoods or SNPs) (**Fig. S3**).

After filtering for genic sites plus 10kb windows, NGSadmix retained 10.5M genotype likelihood sites for admixture analyses in genomes mapped to CanFam3.1 and 9.89M sites for genomes mapped against the African hunting dog. Using the full dataset of 23 genomes, NGSadmix failed to identify a most probable value of K based on the maximum likelihood estimation implemented in the program (Skotte & Albrechtsen, 2013), with high numbers of K receiving the highest likelihood. We extracted and plotted in R the best likelihood values for every K and attempted to find the best-fit K, but the best likelihood was found at very large K values, even beyond the number of individuals included in the analysis (**Fig. S4**). A relative maximum was found at K=21. This issue may indicate sub-clustering within the species studied (Pilot et al., 2019), and does not necessarily mean lack of population structure. Nonetheless, a series of general trends could be identified. Starting from K=6 onwards, the Ethiopian and Kenyan African golden wolves clustered together in a different population from the other AGWs. From K=5 to K=10, the Egyptian AGW appears to have mixed ancestry between African golden wolves and possibly Middle Eastern gray wolves or dogs from Africa (**Fig. 2A**). Notably, at K=9 the Ethiopian AGW seems to share some proportion of

alleles from a postulated ancestral population with Ethiopian wolves, but this trend is not shown at any other K or level of clustering.

When considering African golden wolves alone (**Fig. 2B**), some structure is detected between the southeast population (Ethiopia, Kenya) and the northern population (Algeria, Egypt, Morocco, Senegal). This pattern is consistent with a general trend in big African carnivores and ungulates to cluster in northern and southeast populations divided by the Rift Valley (Bertola et al., 2016; Brown et al., 2007; Charruau et al., 2011; Flagstad, Syvertsen, Stenseth, & Jakobsen, 2001; Lorenzen, Heller, & Siegismund, 2012; Moodley & Bruford, 2007; Muwanika, Nyakaana, Siegismund, & Arctander, 2003; Smitz et al., 2013), and is also consistent with previous studies on African golden wolves (Gopalakrishnan et al., 2018). No mixed composition was detected in the Egyptian individual from other different African golden wolves when no dogs or gray wolves were present at the NGSadmix study. SNP-based Admixture plots showed very similar results, and only small local proportions of admixture between dog and gray wolf were detected when comparing NGSadmix and Admixture plots generated for mapped genomes against CanFam3.1 and African hunting dog (**Fig. S5**). Since we did not detect major reference biases in African golden wolf genomes, all subsequent analyses were performed using autosomes mapped against CanFam3.1.

Complex and heterogeneous demographic history

With PSMC, three possible groups of lineages with similar demographic histories could be seen: one for eastern AGW from Kenya and Ethiopia, another for the Senegalese and Algerian individuals, and another one for the two Moroccan individuals (**Fig. 3**). The Egyptian AGW showed a very steep increase in effective population size (Ne) towards the end of the graph that could be interpreted as introgression and could not be placed with the other samples at the plot.

While the Moroccan lineages could have benefited from a series of GSP identified at 124 kyr (Eemian), ca. 100 kyr and 80 kyr ago (Ehrmann et al., 2017; Larrasoaña et al., 2013), the eastern group showed a relatively constant decrease in population since 300 kyr ago, reaching a minimum Ne of ca. 40,000 at around 45 kyr ago, after which animals from west and east of the Rift Valley follow different demographic trajectories (**Fig. 3**). Both Moroccan lineages seem to have followed a similar trajectory until about 28 kyr ago, after which the west Moroccan lineage has a steep reduction in population effective size, while the east Moroccan lineage remains constant. The Senegalese and Algerian individuals shared a demographic history until about 100 kyr ago, when they diverge, with a constant decrease in population for the Algerian individual and a very steep decrease for the Senegalese lineage after 24kyr ago. Some proposed events of enhanced dry conditions in north Africa driven by Heinrich stadials could have caused decreases in these populations. Heinrich Event 6 (58.25-58.85 kyr ago, Rohling et al., 2003) appears to coincide with a reduction of population size in the Moroccan lineages, while all populations experienced a reduction after Heinrich Event 2 (ca. 23.6-25.9 kyr ago; Rohling et al., 2003) (**Fig. 3**). However, the

resolution for this time is not sufficient to confidently associate climate events with population contractions. Pleistocene climate changes in north Africa did not impact the African golden wolves equally or synchronously across their range.

After 70 kyr ago all lineages, including the Egyptian individual, show an increase in population size according to ngsPSMC (**Fig. 4A**), although at different times. The first lineages to experience this increase are found in the western part of the range, and later in the east when the Kenyan lineage reached an effective population size of more than 16,000 by 28-30 kyr ago (**Fig. 4A**). Strikingly, around 53 kyr ago we observe an increase in population size in the Algerian and Egyptian AGW that can be connected to a local wetter event in the northernmost fringe of the Sahara (Hoffmann et al., 2016). Western populations reached minimum effective population sizes around 30-40 kyr ago (Moroccan individuals), and 35-25 kyr (Algeria, Ethiopia), followed by local recoveries and relative maximums around 15-25 kyr ago. The Kenyan, Egyptian and Senegalese lineages (from the extremes of the distribution) show no recovery after their initial minima.

A general decrease in population sizes was observed from the last part of the last Glacial Maximum (LGM) around 18 kyr ago through the Younger Dryas (YD) with no recoveries during the wetter phase of the Holocene GSP ca. 10-5.5 kyr ago (**Fig. 4B**). Consistent with a differentiation in paleodistribution of these animals, there are general increases of effective population size that start at different times: while the easternmost (Ethiopia, Kenya) lineages reach a local minimum in population size around 3-3.5kyr ago, the northwestern Moroccan lineages experience their minimum more recently at ca. 2.7-3 kyr ago and Senegal and Algeria reach theirs around 2-2.2 kyr ago. The western populations all reach their local maximum around 1000 years ago, to decrease again afterwards (**Fig. 4B**). A final steep increase in population size is seen only in the Egyptian and Kenyan lineages ca. 150 and 90 years ago, respectively. While the first one could be attributed to local hybridization with another species, the Kenyan increase could be the result of two converging lineages of the same species. Our analysis failed to identify any more changes in population size after 70 years ago (ca. 23 generations), and attempts to do so with IBD-based methods did not yield any results.

We observed similar behavior for all four populations in Watterson's theta (Θ_W) (Watterson, 1975), nucleotide diversity ($\Theta\pi$) (Tajima, 1989), and Fu & Li's theta (Θ_{FL}) (Fu & Li, 1993) (**Table 1, Fig. S6A**). Although means showed very similar trends, Fu and Li's (Θ_L) (Fu & Li, 1993) and Fay and Wu's (Θ_H)(Fay & Wu, 2000) thetas were very different between the northwest and eastern African golden wolf populations.

Neutrality tests show very similar results in all four populations considered (**Table 1, Fig. S6B**). While Tajima's D (Tajima, 1989) is negative and very close to zero in northwestern AGW, North American

coyotes and gray wolves from the Middle East; D is positive for eastern AGW, which could be indicative of an ongoing population contraction (Durrett, 2008; Zeng et al., 2006). However, trends were very similar among all populations. These values are not significantly different from zero for a population of four individuals according to Tajima (1989) (-0.876, 2.336, p-value: 0.001) (Tajima, 1989), so the neutral mutation hypothesis could explain the DNA polymorphism of these neutral sites. Fu and Li's D and F are also not significantly different from zero (Fu and Li's D and F intervals: [-1.87, 2.38] and [-1.96, 2.78], α=0.01) (Fu & Li, 1993), so our values are within the normal variation expected under the neutral mutation hypothesis. This is consistent with non-genic data and does not provide evidence for recent population expansions or contractions.

An exception occurs with Fay's H (Fay & Wu, 2000) and Zeng's E (Zeng et al., 2006) neutrality tests. Fay's H was uniformly negative and Zeng's E was uniformly positive in all four populations studied (**Table 1, Fig. S6B**). A slightly higher value for northwestern than eastern African golden wolves was detected in Zeng's E values, which could be representative of a recent population growth (Zeng et al., 2006). However, values for all four populations were very similar and it was difficult to detect major differences. Fay's H trend was slightly higher in eastern than in northwestern African golden wolves, which could be representative of a recent population decline (Fay & Wu, 2000; Zeng et al., 2006). However, all standard deviations overlapped with each other, so they were not significantly different (**Table 1, Fig. S6B**).

We tested whether the three population model of the PSMC plot was consistent for genome wide Fst values across lineages without accounting for genic regions. Surprisingly, the Algerian, east Moroccan and Senegal individuals showed a very low Fst between lineages (0.06-0.09) (**Table 2A**). These Fst values were lower than those found within North American coyote lineages at similar or even shorter geographic distances (**Table 2C**), although we found a greater standard deviation in genome wide values of Fst (**Table S5**). These results were striking considering that coyotes are known for being highly mobile animals, with high rates of heterozygosity and forming populations much closer to panmixia and less affected by isolation by distance than gray wolves (DeCandia et al., 2019; Heppenheimer, Brzeski, et al., 2018; Heppenheimer, Cosio, et al., 2018; Pilot et al., 2006). Although the west Moroccan individual was found less than 1000 km away from the east Moroccan individual, it had large genome wide pairwise F_{ST} values with the east Morocco, Senegal and Algerian individuals (**Table 2A**). Algeria, east Morocco and Senegal individuals showed a fairly similar genetic distance to both east African lineages (Ethiopia and Kenya).

Different histories of inbreeding

We used an SFS-based method to analyze the proportion of singletons with respect to the rest of sites and infer genome wide heterozygosity per individual corrected by genome wide depth

(Gopalakrishnan et al., 2018). We found that African golden wolves had a mean genome wide heterozygosity of $7.83*10^{-4}$ (standard deviation (SD): $1.82*10^{-4}$); closer to North America coyotes ($7.95*10^{-4}$, SD: $9.38*10^{-5}$) than to gray wolves from the Middle East ($6.33*10^{-4}$, SD: $1.89*10^{-4}$) and higher than domestic dogs ($5.17*10^{-4}$, SD: $9.71*10^{-5}$) (**Fig. S7**). However, the west Moroccan individual had a low genome wide heterozygosity ($5.01*10^{-4}$).

Although inbreeding coefficients varied among individuals, the Egyptian, Kenyan and west Moroccan African golden wolves were more inbred than the rest of the individuals of the species (**Table 3**), partially consistent with being at the extremes of the distribution. PLINK and ngsF's estimation of inbreeding coefficient yielded some differences that could be explained by differences in the calculation methods of each software. Our efforts to determine the influence or bias across genomes of varying depths of coverage (7X, 9X, 11.2X and 15-24X) found that ngsF is less sensitive to changes in coverage than PLINK, and tends to overestimate the homozygosity of the Kenyan over the Egyptian individual (**Table S6**). In any case, PLINK also identified the Kenyan, Egyptian, and west Moroccan individuals as the most inbred.

This approach could not be replicated, however, when using ROH-based methods to estimate inbreeding. Except for samples with a high mean genome wide coverage (Kenyan AGW – 26X, Iranian gray wolf – 26X, Californian coyote – 23X), we detected almost no ROHs in AGWs (**Table 3**). ROH-based calculations mostly underestimated Fi ratios detected by both ngsF and PLINK, especially in lower coverage genomes. This failure could be due to the dependency of these methods to detect long stretches with homozygous sites when using low coverage samples, or on the wide variety in methods and thresholds to infer ROHs (Sams & Boyko, 2019).

Using a 50-kb windows-based approach across the west Moroccan AGW and the east Moroccan AGW genomes (**Fig. S8**), we observed several regions where heterozygosity approaches zero in the west Moroccan individual. This trend is especially remarkable when compared with the east Moroccan individual, who only has a single possible ROH in chromosome 11. Furthermore, the Senegal sample (7X coverage) did not show any increased homozygosity as compared to other samples of higher coverage.

The west Moroccan genome is the African golden wolf with the highest inbreeding coefficient observed in this dataset and the east Moroccan is the one with the lowest. This difference between geographically close lineages is remarkable when considering that other lineages more distant from each other share more alleles, have higher rates of heterozygosity, and lower pairwise Fst values (**Table 2A**).

Divergence during glacial periods

We observed highly consistent results in divergence time estimation regardless of genome coverage (see Supplementary File: "Replicability tests: results", **Table S7**). MiSTI also gave coherent results regardless of the time segment definition used (**Table S8**), so we used time segments defining humid/dry

periods of Sahara according to Larrasoaña et al., (2013). Every divergence time estimation was run covering all time steps until 150 kyr ago. We also found good consistency between our MiSTI and Cavalli-Sforza divergence estimates except for those divergence times involving either the Ethiopian or the west Moroccan genomes (**Table S9**), which had the lowest genome wide heterozygosity (see **Table 3**).

We found a recurrent pattern of isolation of local lineages at times corresponding to glacial maxima in the Northern Hemisphere. We failed to detect the splitting time of three lineages (Algeria, Senegal, east Morocco) (**Fig. 5, Table S10**), which is consistent with very low genome wide pairwise Fst values (**Table 2**). Since the last splitting time considered by MiSTI was ca. 3 kyr ago, the separation of east Morocco, Algeria and Senegal lineages (referred to as the EMAS cluster) may have happened very recently (less than 3 kya), or they may maintain geneflow. Splitting times of the EMAS cluster from Egyptian AGW happened around 9-11 kyr ago (**Table 1**), which overlaps or follows the Younger Dryas in north Africa ca. 10-13 kyr ago (Ehrmann et al., 2017).

Most lineage divergences happened between ca. 16 kyr and 30 kyr ago (**Table S10**), overlapping with cold Heinrich stadials (Ehrmann et al., 2017; Heinrich, 1988; Rohling et al., 2003). The west Moroccan lineage diverged from the EMAS cluster ca. 16-21 kyr ago (**Table S10**), overlapping with Heinrich stadial H2 (Ehrmann et al., 2017; Heinrich, 1988; Rohling et al., 2003), as well as the divergence time of Ethiopian and Kenyan lineages, which probably happened around 17.5 kyr ago. The Kenyan lineage shows a more widespread divergence with all other lineages in the north, with a likely splitting time of 22.3 kyr with the EMAS cluster, 24.1 kyr with the Egyptian lineage, and ca. 29.4 kyr with the west Moroccan lineage, which could have followed cooling periods known as Heinrich stadials H2 and H3. Divergence times between the Ethiopian lineage and EMAS cluster and the Egyptian lineage probably happened between 26.9-30.3 kyr ago, coinciding with Heinrich stadial H3 (**Fig. S9B, Table S10**). We have not found any signatures of divergence after the Holocene GSP ca. 10-5.5 kyr ago (Drake et al., 2013; Larrasoaña et al., 2013; Smith, 2012).

After calculating migration rates during time segments, we observe a general trend with increased migration rates at around 80 kyr, 100 kyr and 120 kyr for some lineages, therefore increasing gene flow (**Table S11**). This is consistent with previous paleoclimatological data that point to three GSPs around those periods (Drake et al., 2013; Ehrmann et al., 2017; Larrasoaña et al., 2013; Smith, 2012). Furthermore, we have detected certain periods of increased migration that could coincide with minor wet phases reported at ca 52.5-50.5 kyr and 37.5-33 kyr ago in the northern Sahara (Hoffmann et al., 2016), such as west Morocco → Egypt (35.2-51 kyr) and Senegal → east Morocco (29.9-36.3kyr). However, time segments as defined by PSMC are wide and more resolution is needed to properly infer when these migration rates increased in the past.

DISCUSSION

Climate change-driven differentiation of African golden wolf lineages

Our results indicate that the divergence times of all lineages of African golden wolves occurred during the latest Pleistocene, between 50 and 10.5 kyr ago, with most divergence times clustered between 16 and 30 kyr ago, broadly coinciding with the Late Glacial Maximum (LGM) at ca. 33-16 kyr ago (Clark et al., 2009) (**Fig. 5**). Strikingly, all divergence events are associated to either Heinrich stadials H1 to H4 or to the Younger Dryas, clearly linking divergence times with periods of enhanced dry conditions in the Sahara. We hypothesize that these 1500-year-long drier periods reinforced the isolation of mesic and water-dependent species in refugia (Brito et al., 2014), where isolation during hundreds of generations caused genetic divergence. Although some relative warming and cooling periods have been proposed since the middle Holocene that could be linked to relative changes in population size, the worldwide impact of these local events is heavily debated (Neukom, Steiger, Gómez-Navarro, Wang, & Werner, 2019) and we could not find a direct correlation.

It has been proposed that the onset of wetter conditions during later GSP permitted mesic species to expand and reconnect, a pattern seen in a wide number of species in north Africa (Ben Faleh et al., 2012; Cosson et al., 2005; Lerp et al., 2011; Nicolas et al., 2009; Rato et al., 2007). The last GSP (ca. 10-5.5 kyr ago) reconnected animals isolated in several refugia (Kuper, & Kröpelin, 2006; Linstädter & Kröpelin, 2004; Yeakel et al., 2014). However, we have not detected strong signatures of gene flow between African golden wolf lineages during this period (except for the EMAS cluster), suggesting that this period was not wet enough to erase patterns of genetic differentiation. This is consistent with the drier nature of the Holocene GSP in comparison with previous GSP (Ehrmann et al., 2017).

An exception to this is the east Moroccan AGW. While the west Moroccan population seems to have been isolated for the last 18,000 years and have undergone a high degree of inbreeding, the east Moroccan individual presents one of the highest levels of genome wide heterozygosity and is genetically close to lineages from Senegal and Algeria, forming the EMAS cluster. It is characterized by a wide distribution (3,200 km wide), a relatively recent divergence (less than 3,000 years ago), and the exclusion of the west Moroccan lineage, all of which are intriguing features. African golden wolves are known to have large home ranges (up to 22 km^2 in Kenya, Fuller et al., 1989, and 64.8 km^2 in Ethiopia, Admasu et al., 2004) and large dispersal capabilities (in Tunisia, an individual was detected to have walked 230 km in 98 days, Karssene et al., 2018). A recent study (Eddine et al., 2020) detected almost no genetic structuring in a wide variety of samples from Algeria and Tunisia that encompassed roughly 1,200 km. The east and west Moroccan individuals are less than 1,000 km apart from each other. Why then, would the west

Moroccan individual present such high levels of inbreeding and be isolated from other African golden wolves for nearly 18,000 years?

Atlas: refugium during glacial times

Previous studies (Cosson et al., 2005; Husemann et al., 2014; Leite et al., 2015; Rato et al., 2007) have identified the Atlas Mountains of Maghreb as a glacial refugium during drier times for a variety of species. The highly heterogeneous landscape is formed by several mountain ranges (Anti-Atlas, High Atlas, Middle Atlas, Rif) with some of the highest peaks in north Africa (Jbel Toubkal, 4,165m), deep humid valleys, and relict high mountain cedar forests (Abel-Schaad et al., 2018) with isolated and endangered populations of *Macaca sylvanus* (Ciani et al., 2005) and rivers that act as barriers to arid-adapted species (Rato et al., 2007). These features are key for the establishment of "refugia within refugia", with high endemism, barriers that subdivide habitats and the potential for genetic divergence and speciation (Dufresnes et al., 2020; Gómez & Lunt, 2007).

The isolation of the west Moroccan lineage could have arisen in a variety of ways. The 'rear edge hypothesis' of Hampe & Petit (2005) proposes a scenario where previously isolated demes in interglacial refugia converge in an admixture zone, leaving behind groups that have undergone local adaptations in response to abiotic stresses. This could explain why the east Moroccan individual appears to have merged with the Algerian and Senegalese lineages in recent times, even though the demographic histories of the west and east Moroccan individuals appear overlapped until 60,000 years ago (**Fig. 3**). In this scenario, the west Moroccan lineage could be one of the groups from the rear edge that failed to reconnect with others. Hampe and Petit (2005) explain how relict populations are not necessarily the source of postglacial expansions and this could be the case of the west Moroccan lineage.

Another possibility is that the west Moroccan lineage belongs to a population that has not contributed to the EMAS cluster for thousands of years. In a previous study on red fox (*Vulpes vulpes*), Leite et al. (2015) detected two main lineages in northwestern Africa: animals from Atlantic Sahara to Tunisia (Maghreb 1) and a more isolated lineage restricted to the valley of Oukaimeden, north of the High Atlas Mountains (Maghreb 2). The west Moroccan individual was found north of the High Atlas, which is the tallest mountain range of the Atlas Mountains (over 4000 m high) and could have restricted movements of African golden wolves. However, African golden wolves have been observed living at medium to high elevations (2,000-3,000m) in Algeria (Amroun et al., 2014), Ethiopia (Admasu et al., 2004; Gaubert et al., 2012; Rueness et al., 2011; Simeneh, 2010), Tanzania (Temu, Nahonyo, & Moehlman, 2018), and Morocco (Cuzin, 2003; Urios et al., 2015; Waters, Harrad, Amhaouch, Taiqui, & Senn, 2015). There is a possibility, therefore, that the west Moroccan lineage represents a different, adapted ecotype of the same species of African golden wolf, parallel to what has been seen with North American gray wolves, where ecology

drives differentiation in local populations (Leonard, 2014). Further studies and more sampling across the High Atlas Mountains will reveal whether African golden wolves follow a localized pattern of specialized demes associated with different ecosystems.

Recent admixture in the EMAS cluster

In a previous study based on 13 autosomal microsatellites and mitochondrial control region sequences, Eddine et al. (2020) failed to identify structure between Algerian and Tunisian African golden wolves, and estimated an increase in population size between 3,840 and 6,720 years ago. However, across this time period we found an almost constant decrease of population size with ngsPSMC (**Fig. 4B**). Higher values of Θ_H indicate a greater abundance of high-frequency variants than in northwest AGW, which could suggest a high number of shared variants among the northwestern individuals and possible recent gene flow between different lineages of wolves. In contrast, eastern AGW show a lower abundance of high frequency variants, which is possibly indicative of a process of local divergence of the two lineages in the region (Ethiopia, Kenya).

The high genome wide heterozygosity observed in the EMAS cluster could come from a recent admixture of distant lineages (as we failed to detect a divergence time using MiSTI), increasing genetic variability. Previous work in red fox also detected a widespread lineage that extended from Atlantic Sahara to Tunisia (Leite et al., 2015). Allele-based estimations of Ne have been found to be affected by recent admixture processes in human populations (Lohmueller, Bustamante, & Clark, 2010) and recent studies have focused on independently ascertaining demographic histories of genomic portions of diverse origin in admixed individuals (Browning & Browning, 2015; Browning et al., 2018; Skov et al., 2020). Future IBD-based studies of whole genomes of individuals from the EMAS cluster could help disentangle the hypotheses of a recent Neolithic expansion versus a recent admixture that enriched the diversity of local demes.

Dynamic demographic histories

With PSMC we have found a complex demographic history, where lineages do not follow the same trends of expansion or contraction through time (**Fig. 3**). This could be due to a variety of causes. First, current lineage locations might not represent those of the past. Consistent with the detected pattern in the west Moroccan sample, other lineages might have remained isolated for thousands of generations in a refugium and not have contributed for several GSP to the postglacial admixed populations, therefore increasing genome wide inbreeding and decreasing Ne.

Second, GSP did not lead to homogeneous savannah landscapes throughout the desert, a circumstance that has been shown for the two GSP for which more paleoenvironmental evidence is available (Eemian, ca. 122-128. kyr ago; and Holocene, 5.5-10 kyr ago). Complex topography modulated

the S-N and W-E gradient of decreasing monsoonal rainfall, thereby creating areas of more or less aridity with different environments (Larrasoaña et al., 2013). With such a heterogeneous landscape, mild GSP would not have had much impact on local populations closer to arid zones while other populations would have benefitted from more humid environments. Different refugia within the Sahara could have hosted distinct populations of African golden wolves with diverse reactions to climate change. Further, competitive pressure from black-backed jackals (Van Valkenburgh & Wayne, 1994) and/ or hyaenas (Kebede et al., 2017; Kingdon, 2013) may not have been equal throughout the entire Sahara region if their past distributions were not entirely overlapping with the distribution of African golden wolves.

A third possibility is that we are detecting different ecotypes of the same species. In gray wolves, the onset of postglacial conditions benefited some populations, while others, possibly adapted to colder conditions and/ or bigger prey, declined or went extinct (Ersmark et al., 2016; Leonard et al., 2007). Although current African golden wolves are generalist predators and maintain a varied diet composed of small mammals, birds, plants, insects and waste (Amroun et al., 2014; Amroun et al., 2006; McShane & Grettenberger, 1984), predation of gazelles has been detected in Niger, Kenya and Tanzania (Fuller et al., 1989; McShane & Grettenberger, 1984; Moehlman, 1986; Temu, Nahonyo, & Moehlman, 2016; Temu et al., 2018). It is unknown if the decline of gazelles after ca. 25 kyr ago (Lerp et al., 2011) impacted local populations of AGW, or if some of them were more specialized predators of ungulates. Another factor is habitat preference. While African golden wolves have been detected in all sorts of environments in Algeria (Amroun et al., 2014; Amroun et al., 2006), Tunisia (Karssene, Chammem, Khorchani, Nouira, & Li, 2017; Karssene et al., 2018), Morocco (Cuzin, 2003) and Niger (McShane & Grettenberger, 1984), some prefer farmlands and covered woodlands over open environments in Ethiopia (Admasu et al., 2004; Simeneh, 2010). In places where AGW are sympatric with competitors such as black-backed jackals, they are found mostly in open grasslands and rarely in woodlands (Fuller et al., 1989; Moehlman, 1986). Human pressure is another important factor to take into consideration. African golden wolves are found close to highly anthropized zones in Algeria and Ethiopia (Admasu et al., 2004; Amroun et al., 2014; Amroun et al., 2006; Simeneh, 2010), while they tend to avoid humans in Morocco, where higher human pressures exist (Brito et al., 2014; Cuzin, 2003). While it has been proposed that increasing anthropization could have driven a recent population expansion in northeast Africa either through the arrival of caprid livestock or through predator control (Eddine et al., 2020), almost negligible amounts of livestock remains were found in fecal diet studies in Niger, Tanzania and Ethiopia (Admasu et al., 2004; Fuller et al., 1989; McShane & Grettenberger, 1984; Simeneh, 2010). It remains plausible to consider that different abiotic and biotic factors could have driven different populations of African golden wolf to specialize into ecotypes. It is unknown whether current African golden wolves arose from bottlenecked specialized ecotypes from the past, but it is a possibility that cannot be excluded.

In this study we sampled the extremes of the distribution that were most probably not directly (re)connected (with the exception of the EMAS cluster) after the Younger Dryas; however, "jackal-like" forms have been discovered in several archaeological sites with dates closer to Holocene GSP conditions (di Lernia, 1998; Guagnin, 2015; Sereno et al., 2008) that could indicate higher connectivity among locations that we have not detected with our dataset. A higher number of samples from more diverse locations -and possibly, historic or ancient DNA – could ascertain whether extinct ecotypes of African golden wolf roamed the once green Sahara landscape.

Speciation and the mid-Pleistocene transition

The mid-Pleistocene transition was characterized by the shift of 41 kyr long glacial-interglacial cycles to much longer and more intense 100 kyr long glacial-interglacial cycles (McClymont et al., 2013) and a general trend of increased aridity in northern Africa (DeMenocal, 2004; Trauth, Larrasoaña, & Mudelsee, 2009). Based on genetic evidence, two studies suggested a date of 1.32 million years ago (Ma) for the speciation event that gave rise to AGW, with a confidence interval of either 1.0-1.65 Ma (Koepfli et al., 2015) or 1.1-1.5 Ma (Chavez et al., 2019). This may be consistent with the oldest "jackal-like" fossils referred to as golden jackals (*Canis aureus*) dating back to the Middle Pleistocene in Morocco (Geraads, 2011). Overall, these data suggest that a shift to enhanced aridity in the Sahara at 1.44 +/- 0.2 Ma (Trauth et al., 2009) drove the speciation of African golden wolves (**Fig. 6**) (Chavez et al., 2019; Koepfli et al., 2015) and reinforces the view that the mid-Pleistocene transition was a prime driver of speciation events in north Africa (DeMenocal, 2004). The increase of aridity ca. 1.2-1.4 Ma also coincides with the expansion and formation of new haplogroups of scimitar-horned onyx (Iyengar et al., 2007), the appearance of several clades of rodents (*Praomys rostratus*; Nicolas et al., 2008; genus *Acomys;* Nicolas et al., 2009; desert-adapted *Gerbillus tarabuli*, Ndiaye et al., 2011) and the divergence of red foxes and Rueppell foxes, the latter being a species more adapted to arid conditions (Leite et al., 2015). In east Africa, the mid-Pleistocene transition is suggested to be connected to the appearance of modern carnivores, especially those of the genus *Canis* (Werdelin & Lewis, 2005)

ACKNOWLEDGEMENTS

We are grateful to I. Salado, S. Ravagni, A. Cornellas and M. Camacho-Sánchez for their assistance in lab work and in the analyses. Logistical support was provided by Laboratorio de Ecología Molecular (LEM-EBD) and by the infrastructures offered by Doñana's Singular Scientific-Technical Infrastructure (ICTS-EBD). Informatic technical support was provided by the High-Performance Computing (HPC) Research Center in Princeton University. CS was supported by a PhD fellowship from Programa Internacional de Becas "La Caixa-Severo Ochoa" of the Spanish Ministerio de Economía y

Competitividad and La Caixa bank (BES-2015-074331). This project was funded by the Frontera grant P18-FR-5099 from the Junta de Andalucia. EBD-CSIC received support from the Spanish Ministry of Economy and Competitiveness under the 'Centro de Excelencia Severo Ochoa 2013-2017' program, SEV-2012-0262.

AUTHOR CONTRIBUTIONS

J.A.L. developed the initial concept which was further developed with C.S. and B.V.H. V.U. provided the sample of the west Moroccan African golden wolf. C.S. conducted data analyses. B.V.H. and J.A.L. assisted with interpretation of genomic results. J.C.L. assisted with interpretation of paleoclimatological results. All authors discussed the results and provided edits and approval of the manuscript.

DATA AVAILABILITY STATEMENT

All data generated in this study have been made available in Github: https://github.com/cdomsar/DivgLupaster. Newly sequenced African golden wolf has been deposited into EMBL-EBI server under accession number ERP123054.

REFERENCES

Abel-Schaad, D., Iriarte, E., López-Sáez, J. A., Pérez-Díaz, S., Sabariego Ruiz, S., Cheddadi, R., & Alba-Sánchez, F. (2018). Are Cedrus atlantica forests in the Rif Mountains of Morocco heading towards local extinction? *Holocene*, *28*(6), 1023–1037. https://doi.org/10.1177/0959683617752842

Abraham, G., & Inouye, M. (2014). Fast principal component analysis of large-scale genome-wide data. *PLoS ONE*, *9*(4), 1–5. https://doi.org/10.1371/journal.pone.0093766

Admasu, Ermias, Thirgood, S. J., Bekele, A., & Karen Laurenson, M. (2004). Spatial ecology of golden jackal in farmland in the Ethiopian Highlands. *African Journal of Ecology*, *42*(2), 144–152. https://doi.org/10.1111/j.1365-2028.2004.00497.x

Alexander, D. H., Novembre, J., & Lange, K. (2009). Fast model-based estimation of ancestry in unrelated individuals. *Genome Research*, *19*(9), 1655–1664. https://doi.org/10.1101/gr.094052.109

Amroun, M, Oubellil, D., & Gaubert, P. (2014). Trophic ecology of the Golden Jackal in Djurdjura National Park (Kabylie, Algeria) . *Revue d'Ecologie (La Terre et La Vie)*, *69*(3–4), 304–317.

Amroun, Mansour, Bensidhoum, M., Delattre, P., & Gaubert, P. (2014). Feeding habits of the common genet (genetta genetta) in the area of djurdjura, north of Algeria. *Mammalia*, *78*(1), 35–43. https://doi.org/10.1515/mammalia-2012-0111

Amroun, Mansour, Giraudoux, P., & Delattre, P. (2006). A comparative study of the diets of two sympatric carnivores - The golden jackal (Canis aureus) and the common genet (Genetta genetta) - In Kabylia, Algeria. *Mammalia*, *70*(3–4), 247–254. https://doi.org/10.1515/MAMM.2006.040

Andrews, S. (2010). *FastQC: a quality control tool for high throughput sequence data.* Available online at: http://www.bioinformatics.babraham.ac.uk/projects/fastqc.

Aulagnier, S. (1992). *Zoogéographie des mammifères du Maroc : de l'analyse spécifique à la typologie de peuplement à l'échelle régionale*. (PhD thesis). Université des sciences et techniques de Montpellier 2.

Auton, A., Rui Li, Y., Kidd, J., Oliveira, K., Nadel, J., Holloway, J. K., … Boyko, A. R. (2013). Genetic Recombination Is Targeted towards Gene Promoter Regions in Dogs. *PLoS Genetics*, *9*(12). https://doi.org/10.1371/journal.pgen.1003984

Barbato, M., Orozco-terWengel, P., Tapio, M., & Bruford, M. W. (2015). SNeP: A tool to estimate trends in recent effective population size trajectories using genome-wide SNP data. *Frontiers in Genetics*, *6*(MAR), 1–6. https://doi.org/10.3389/fgene.2015.00109

685 Ben Faleh, A., Granjon, L., Tatard, C., Boratyński, Z., Cosson, J. F., & Said, K. (2012). Phylogeography of
686 two cryptic species of African desert jerboas (Dipodidae: Jaculus). *Biological Journal of the Linnean*
687 *Society*, *107*(1), 27–38. https://doi.org/10.1111/j.1095-8312.2012.01920.x

688 Bertola, L. D., Jongbloed, H., Van Der Gaag, K. J., De Knijff, P., Yamaguchi, N., Hooghiemstra, H., … De
689 Iongh, H. H. (2016). Phylogeographic Patterns in Africa and High Resolution Delineation of Genetic
690 Clades in the Lion (Panthera leo). *Scientific Reports*, *6*(May 2015), 1–11.
691 https://doi.org/10.1038/srep30807

692 Bolfíková, B. Č., Eliášová, K., Loudová, M., Kryštufek, B., Lymberakis, P., Sándor, A. D., & Hulva, P.
693 (2017). Glacial allopatry vs. postglacial parapatry and peripatry: The case of hedgehogs. *PeerJ*,
694 *2017*(4), 1–21. https://doi.org/10.7717/peerj.3163

695 Brito, J. C., Godinho, R., Martínez-Freiría, F., Pleguezuelos, J. M., Rebelo, H., Santos, X., … Carranza, S.
696 (2014). Unravelling biodiversity, evolution and threats to conservation in the sahara-sahel. *Biological*
697 *Reviews*, *89*(1), 215–231. https://doi.org/10.1111/brv.12049

698 Brown, D., Brenneman, R., Koepfli, K., Pollinger, J., Mila, B., Georgiadis, N., … Wayne, R. (2007).
699 Extensive population genetic structure in the giraffe. *BMC Biology*, *5*(57).
700 https://doi.org/10.1186/1741-7007-5-57

701 Browning, S. R., & Browning, B. L. (2015). Accurate Non-parametric Estimation of Recent Effective
702 Population Size from Segments of Identity by Descent. *American Journal of Human Genetics*, *97*(3),
703 404–418. https://doi.org/10.1016/j.ajhg.2015.07.012

704 Browning, S. R., Browning, B. L., Daviglus, M. L., Durazo-Arvizu, R. A., Schneiderman, N., Kaplan, R.
705 C., & Laurie, C. C. (2018). Ancestry-specific recent effective population size in the Americas. *PLoS*
706 *Genetics*, *14*(5), 1–22. https://doi.org/10.1371/journal.pgen.1007385

707 Camacho-Sanchez, M., Quintanilla, I., Hawkins, M. T. R., Tuh, F. Y. Y., Wells, K., Maldonado, J. E., &
708 Leonard, J. A. (2018). Interglacial refugia on tropical mountains: Novel insights from the summit rat
709 (Rattus baluensis), a Borneo mountain endemic. *Diversity and Distributions*, *24*, 1252–1266.
710 https://doi.org/10.1111/ddi.12761

711 Campana, M. G., Parker, L. D., Hawkins, M. T. R., Young, H. S., Helgen, K. M., Szykman Gunther, M., …
712 Fleischer, R. C. (2016). Genome sequence, population history, and pelage genetics of the endangered
713 African wild dog (Lycaon pictus). *BMC Genomics*, *17*(1), 1–10. https://doi.org/10.1186/s12864-016-
714 3368-9

715 Castañeda, I. S., Mulitza, S., Schefuß, E., Lopes, R. A., Damste, J. S. S., & Schouten, S. (2009). Wet
716 phases in the Sahara / Sahel region and human migration patterns in North Africa. *Proceedings of the*
717 *National Academy of Sciences of the United States of America, 106*(48), 20159–20163.

718 Cavalli-Sforza, L. L. (1969). Human diversity. *Proc. 12th Int.Congr. Genet*. 2:405-416

719 Cerling, T. E., Wynn, J. G., Andanje, S. A., Bird, M. I., Korir, D. K., Levin, N. E., … Remien, C. H.
720 (2011). Woody cover and hominin environments in the past 6-million years. *Nature*, *476*(7358), 51–
721 56. https://doi.org/10.1038/nature10306

722 Charruau, P., Fernandes, C., Orozco-Terwengel, P., Peters, J., Hunter, L., Ziaie, H., … Burger, P. A.
723 (2011). Phylogeography, genetic structure and population divergence time of cheetahs in Africa and
724 Asia: Evidence for long-term geographic isolates. *Molecular Ecology*, *20*(4), 706–724.
725 https://doi.org/10.1111/j.1365-294X.2010.04986.x

726 Chavez, D. E., Gronau, I., Hains, T., Kliver, S., Koepfli, K.-P., & Wayne, R. K. (2019). Comparative
727 genomics provides new insights into the remarkable adaptations of the African wild dog (*Lycaon*
728 *pictus*). *Scientific Reports*, *9*(1), 8329. https://doi.org/10.1038/s41598-019-44772-5

729 Ciani, A. C., Palentini, L., Arahou, M., Martinoli, L., Capiluppi, C., & Mouna, M. (2005). Population
730 decline of *Macaca sylvanus* in the middle atlas of Morocco. *Biological Conservation*, *121*(4), 635–
731 641. https://doi.org/10.1016/j.biocon.2004.06.009

732 Clark, P. U., Dyke, A. S., Shakun, J. D., Carlson, A. E., Clark, J., Wohlfarth, B., … McCabe, A. M. (2009).
733 The Last Glacial Maximum. *Science*, *325*(5941), 710–714. https://doi.org/10.1126/science.1172873

734 Cosson, J. F., Hutterer, R., Libois, R., Sarà, M., Taberlet, P., & Vogel, P. (2005). Phylogeographical
735 footprints of the Strait of Gibraltar and Quaternary climatic fluctuations in the western Mediterranean:
736 A case study with the greater white-toothed shrew, *Crocidura russula* (Mammalia: Soricidae).
737 *Molecular Ecology*, *14*(4), 1151–1162. https://doi.org/10.1111/j.1365-294X.2005.02476.x

738 Cuzin, F. (2003). *Les grands mammiferes du maroc meridional*. (PhD thesis) Université des sciences et
739 techniques de Montpellier 2.

740 DeCandia, A. L., Henger, C. S., Krause, A., Gormezano, L. J., Weckel, M., Nagy, C., … vonHoldt, B. M.
741 (2019). Genetics of urban colonization: neutral and adaptive variation in coyotes (Canis latrans)
742 inhabiting the New York metropolitan area . *Journal of Urban Ecology*, *5*(1), 1–12.
743 https://doi.org/10.1093/jue/juz002

744 DeMenocal, P. B. (2004). African climate change and faunal evolution during the Pliocene-Pleistocene.
745 *Earth and Planetary Science Letters*, *220*(1–2), 3–24. https://doi.org/10.1016/S0012-821X(04)00003-
746 2

747 di Lernia, S. (1998). Cultural control over wild animals during the early Holocene: The case of Barbary
748 sheep in central Sahara. In Savino di Lernia & G. Manzi (Eds.), *Before Food Production in North*
749 *Africa* (Vol. 1, pp. 113–126).

750 Dinis, M., Merabet, K., Martínez-Freiría, F., Steinfartz, S., Vences, M., Burgon, J. D., … Velo-Antón, G.
751 (2019). Allopatric diversification and evolutionary melting pot in a North African Palearctic relict:
752 The biogeographic history of Salamandra algira. *Molecular Phylogenetics and Evolution*, *130*(May
753 2018), 81–91. https://doi.org/10.1016/j.ympev.2018.10.018

754 Dobson, M., & Wright, A. (2000). Faunal relationships and zoogeographical affinities of mammals in
755 north-west Africa. *Journal of Biogeography*, *27*(2), 417–424. https://doi.org/10.1046/j.1365-
756 2699.2000.00384.x

757 Drake, N. A., El-Hawat, A. S., Turner, P., Armitage, S. J., Salem, M. J., White, K. H., & McLaren, S.
758 (2008). Palaeohydrology of the Fazzan Basin and surrounding regions: The last 7 million years.
759 *Palaeogeography, Palaeoclimatology, Palaeoecology*, *263*(3–4), 131–145.
760 https://doi.org/10.1016/j.palaeo.2008.02.005

761 Drake, Nick A., Blench, R. M., Armitage, S. J., Bristow, C. S., & White, K. H. (2011). Ancient
762 watercourses and biogeography of the Sahara explain the peopling of the desert. *Proceedings of the*
763 *National Academy of Sciences of the United States of America*, *108*(2), 458–462.
764 https://doi.org/10.1073/pnas.1012231108

765 Drake, Nick A., Breeze, P., & Parker, A. (2013). Palaeoclimate in the Saharan and Arabian Deserts during
766 the Middle Palaeolithic and the potential for hominin dispersals. *Quaternary International*, *300*, 48–
767 61. https://doi.org/10.1016/j.quaint.2012.12.018

768 Dufresnes, C., Nicieza, A. G., Litvinchuk, S. N., Rodrigues, N., Jeffries, D. L., Vences, M., … Martínez-
769 Solano, Í. (2020). Are glacial refugia hotspots of speciation and cytonuclear discordances? Answers
770 from the genomic phylogeography of Spanish common frogs. *Molecular Ecology*, *29*(5), 986–1000.
771 https://doi.org/10.1111/mec.15368

772 Durrett, R. (2008). Probability Models for DNA Sequence Evolution, Second Edition by Richard Durrett.
773 In *Springer*. https://doi.org/10.1111/j.1751-5823.2009.00085_5.x

774 Eddine, A., Mostefai, N., Rocha, R. G., Karssene, Y., De Smet, K., Brito, J. C., … Godinho, R. (2020).
775 Demographic expansion of an African opportunistic carnivore during the Neolithic revolution.
776 *Biology Letters*, *16*(20190560), 1–7.

777 Ehrmann, W., Schmiedl, G., Beuscher, S., & Krüger, S. (2017). Intensity of african humid periods
778 estimated from saharan dust fluxes. *PLoS ONE*, *12*(1), 1–18.
779 https://doi.org/10.1371/journal.pone.0170989

780 Emeis, K. C., Sakamoto, T., Wehausen, R., & Brumsack, H. J. (2000). The sapropel record of the eastern
781 Mediterranean Sea - Results of Ocean Drilling Program Leg 160. *Palaeogeography,*
782 *Palaeoclimatology, Palaeoecology*, *158*(3–4), 371–395. https://doi.org/10.1016/S0031-
783 0182(00)00059-6

784 Ersmark, E., Klütsch, C. F. C., Chan, Y. L., Sinding, M. H. S., Fain, S. R., Illarionova, N. A., …
785 Savolainen, P. (2016). From the past to the present: Wolf phylogeography and demographic history
786 based on the mitochondrial control region. *Frontiers in Ecology and Evolution*, *4*(DEC), 1–12.
787 https://doi.org/10.3389/fevo.2016.00134

788 Fay, J. C., & Wu, C. I. (2000). Hitchhiking under positive Darwinian selection. *Genetics*, *155*(3), 1405–
789 1413.

790 Feliner, G. N. (2011). Southern European glacial refugia: A tale of tales. *Taxon*, *60*(2), 365–372.
791 https://doi.org/10.1002/tax.602007

792 Flagstad, Syvertsen, P. O., Stenseth, N. C., & Jakobsen, K. S. (2001). Environmental change and rates of
793 evolution: The phylogeographic pattern within the hartebeest complex as related to climatic variation.
794 *Proceedings of the Royal Society B: Biological Sciences*, *268*(1468), 667–677.
795 https://doi.org/10.1098/rspb.2000.1416

796 Frantz, L.A.F., Mullin, V.E., Pionnier-Capitan, M., Lebrasseur, O., Ollivier, M., Perri, A., Linderholm, A.,
797 Mattiangeli, V., Teasdale, M.D., Dimopoulos, E.A. (2016). Genomic and archaeological evidence
798 suggest a dual origin of domestic dogs. *Science* 352(6290):1228–1231.

799 Freedman, A. H., Gronau, I., Schweizer, R. M., Ortega-Del Vecchyo, D., Han, E., Silva, P. M., …
800 Novembre, J. (2014). Genome Sequencing Highlights the Dynamic Early History of Dogs. *PLoS*
801 *Genetics*, *10*(1). https://doi.org/10.1371/journal.pgen.1004016

802 Fu, Y. X., & Li, W.-H. H. (1993). Statistical Tests of Neutrality of Mutations. *Genetics*, *133*(3), 693–709.

803 Fuller, T. K., Biknevicius, A. R., Kat, P. W., Van Valkenburgh, B., & Wayne, R. K. (1989). the Ecology of
804 3 Sympatric Jackal Species in the Rift-Valley of Kenya. *African Journal of Ecology*, *27*(4), 313–323.
805 https://doi.org/10.1111/j.1365-2028.1989.tb01025.x

806 Fumagalli, M., Vieira, F. G., Linderoth, T., & Nielsen, R. (2014). NgsTools: Methods for population
807 genetics analyses from next-generation sequencing data. *Bioinformatics*, *30*(10), 1486–1487.
808 https://doi.org/10.1093/bioinformatics/btu041

809 Gaubert, P., Bloch, C., Benyacoub, S., Abdelhamid, A., Pagani, P., Djagoun, C. A. M. S., … Dufour, S.
810 (2012). Reviving the african wolf canis lupus lupaster in north and west africa: A mitochondrial
811 lineage ranging more than 6,000 km wide. *PLoS ONE*, *7*(8).
812 https://doi.org/10.1371/journal.pone.0042740

813 Geraads, D. (2011). A revision of the fossil Canidae (Mammalia) of north-western Africa. *Palaeontology*,
814 *54*(2), 429–446. https://doi.org/10.1111/j.1475-4983.2011.01039.x

815 Geyh, M. A., & Thiedig, F. (2008). The Middle Pleistocene Al Mahrúqah Formation in the Murzuq Basin,
816 northern Sahara, Libya evidence for orbitally-forced humid episodes during the last 500,000 years.
817 *Palaeogeography, Palaeoclimatology, Palaeoecology*, *257*(1–2), 1–21.
818 https://doi.org/10.1016/j.palaeo.2007.07.001

819 Gómez, A., & Lunt, D. H. (2007). Refugia within Refugia: Patterns of Phylogeographic Concordance in the
820 Iberian Peninsula. *Phylogeography of Southern European Refugia: Evolutionary Perspectives on the*
821 *Origins and Conservation of European Biodiversity*, 155–188. https://doi.org/10.1007/1-4020-4904-
822 8_5

823 Gopalakrishnan, S., Sinding, M. H. S., Ramos-Madrigal, J., Niemann, J., Samaniego Castruita, J. A.,
824 Vieira, F. G., … Gilbert, M. T. P. (2018). Interspecific Gene Flow Shaped the Evolution of the Genus
825 Canis. *Current Biology*, *28*(21), 3441-3449.e5. https://doi.org/10.1016/j.cub.2018.08.041

826 Guagnin, M. (2015). Animal engravings in the central Sahara: A proxy of a proxy. *Environmental*
827 *Archaeology*, *20*(1), 52–65. https://doi.org/10.1179/1749631414Y.0000000026

828 Hampe, A., & Petit, R. J. (2005). Conserving biodiversity under climate change: The rear edge matters.
829 *Ecology Letters*, *8*(5), 461–467. https://doi.org/10.1111/j.1461-0248.2005.00739.x

830 Hawkins, M. T. R., Culligan, R. R., Frasier, C. L., Dikow, R. B., Hagenson, R., Lei, R., & Louis, E. E.
831 (2018). Genome sequence and population declines in the critically endangered greater bamboo lemur
832 (Prolemur simus) and implications for conservation. *BMC Genomics*, *19*(1), 1–15.
833 https://doi.org/10.1186/s12864-018-4841-4

834 Heinrich, H. (1988). Origin and consequences of cyclic ice rafting in the Northeast Atlantic Ocean during
835 the past 130,000 years. *Quaternary Research*, *29*(2), 142–152.

836 Hemming, S. R. (2004). Heinrich events: Massive late Pleistocene detritus layers of the North Atlantic and
837 their global climate imprint. *Reviews of Geophysics*, *42*(1). https://doi.org/10.1029/2003RG000128

838 Heppenheimer, E., Brzeski, K. E., Hinton, J. W., Patterson, B. R., Rutledge, L. Y., DeCandia, A. L., …
839 vonHoldt, B. M. (2018). High genomic diversity and candidate genes under selection associated with
840 range expansion in eastern coyote (Canis latrans) populations. *Ecology and Evolution*, *8*(24), 12641–
841 12655. https://doi.org/10.1002/ece3.4688

842 Heppenheimer, E., Cosio, D. S., Brzeski, K. E., Caudill, D., Van Why, K., Chamberlain, M. J., …
843 Vonholdt, B. (2018). Demographic history influences spatial patterns of genetic diversityin recently
844 expanded coyote (Canis latrans) populations. *Heredity*, *120*(3), 183–195.
845 https://doi.org/10.1038/s41437-017-0014-5

846 Hewitt, G. (2000). The genetic legacy of the quaternary ice ages. *Nature*, *405*(6789), 907–913.
847 https://doi.org/10.1038/35016000

848 Hewitt, G. M. (1999). Post-glacial re-colonization of European biota. *Biological Journal of the Linnean*
849 *Society*, *68*(1–2), 87–112. https://doi.org/10.1006/bijl.1999.0332

850 Hoffmann, D. L., Rogerson, M., Spötl, C., Luetscher, M., Vance, D., Osborne, A. H., … Moseley, G. E.
851 (2016). Timing and causes of North African wet phases during the last glacial period and implications
852 for modern human migration. *Scientific Reports*, *6*(September), 1–7.
853 https://doi.org/10.1038/srep36367

854 Husemann, M., Schmitt, T., Zachos, F. E., Ulrich, W., & Habel, J. C. (2014). Palaearctic biogeography
855 revisited: Evidence for the existence of a North African refugium for Western Palaearctic biota.
856 *Journal of Biogeography*, *41*(1), 81–94. https://doi.org/10.1111/jbi.12180

857 Iyengar, A., Gilbert, T., Woodfine, T., Knowles, J. M., Diniz, F. M., Brenneman, R. A., … MacLean, N.
858 (2007). Remnants of ancient genetic diversity preserved within captive groups of scimitar-horned
859 oryx (Oryx dammah). *Molecular Ecology*, *16*(12), 2436–2449. https://doi.org/10.1111/j.1365-
860 294X.2007.03291.x

861 Karssene, Y., Chammem, M., Khorchani, T., Nouira, S., & Li, F. (2017). Global warming drives changes in
862 carnivore communities in the North Sahara desert. *Climate Research*, *72*, 153–162.

863 Karssene, Y., Chammem, M., Nowak, C., de Smet, K., Castro, D., Eddine, A., … Godinho, R. (2018).
864 Noninvasive genetic assessment provides evidence of extensive gene flow and possible high

movement ability in the African golden wolf. *Mammalian Biology*, *92*, 94–101. https://doi.org/10.1016/j.mambio.2018.05.002

Karssene, Y., Nowak, C., Chammem, M., Cocchiararo, B., & Nouira, S. (2019). Genetic diversity of the genus Vulpes (Red fox and Fennec fox) in Tunisia based on mitochondrial DNA and noninvasive DNA sampling. *Mammalian Biology*, *96*, 118–123. https://doi.org/10.1016/j.mambio.2018.09.008

Kebede, Y., Sciences, C., Box, P. O., & Sodo, W. (2017). *A Review on: Distribution, Ecology and Status of Golden Jackal (canis aureus) in Africa*. *7*(1), 32–43.

Kent, J., Charles, S., Sugnet, C. W., Furey, T. S., Roskin, K. M., Pringle, T. H., … Haussler, D. (2002). The human genome browser at UCSC. *Genome Research*, *12*(6), 996–1006. https://doi.org/10.1101/gr.229102.

Kim, H. L., Ratan, A., Perry, G. H., Montenegro, A., Miller, W., & Schuster, S. C. (2014). Khoisan hunter-gatherers have been the largest population throughout most of modern-human demographic history. *Nature Communications*, *5*. https://doi.org/10.1038/ncomms6692

Kingdon, J. (2013). Mammals of Africa. In *Bloomsbury Natural History* (Vol. 50). https://doi.org/10.5860/choice.50-4188

Koch, E. M., Schweizer, R. M., Schweizer, T. M., Stahler, D. R., Smith, D. W., Wayne, R. K., & Novembre, J. (2019). De Novo Mutation Rate Estimation in Wolves of Known Pedigree. *Molecular Biology and Evolution*, *36*(11), 2536–2547. https://doi.org/10.1093/molbev/msz159

Koepfli, K. P., Pollinger, J., Godinho, R., Robinson, J., Lea, A., Hendricks, S., … Wayne, R. K. (2015). Genome-wide evidence reveals that African and Eurasian golden jackals are distinct species. *Current Biology*, *25*(16), 2158–2165. https://doi.org/10.1016/j.cub.2015.06.060

Kuper, R., Kröpalin, S., Kröpelin, S., & Kröpalin, S. (2006). Climate-controlled Holocene occupation in the Sahara: Motor of Africa's evolution. *Science*, *313*(5788), 803–807. https://doi.org/10.1126/science.1130989

Larrasoaña, J. C., Roberts, A. P., Rohling, E. J., Winklhofer, M., & Wehausen, R. (2003). Thre million years of monsoon variability over the northern Sahara. *Climate Dynamics, 21*. 689–698. Https://doi.org/10.1007/s00382-033-0355-z

Larrasoaña, J. C., Roberts, A. P., & Rohling, E. J. (2013). Dynamics of Green Sahara Periods and Their Role in Hominin Evolution. *PLoS ONE*, *8*(10). https://doi.org/10.1371/journal.pone.0076514

Leite, J. V. J. V., Álvares, F., Velo-Antón, G., Brito, J. C. J. C., Godinho, R., Alvares, F., … Godinho, R. (2015). Differentiation of North African foxes and population genetic dynamics in the desert. Insights

into the evolutionary history of two sister taxa, Vulpes rueppellii and Vulpes vulpes. *Organisms Diversity and Evolution*, *15*(4), 731–745. https://doi.org/10.1007/s13127-015-0232-8

Leonard, J. A. (2014). Ecology drives evolution in grey wolves. *Evolutionary Ecology Research*, *16*(6), 461–473.

Leonard, J. A., Vila, C., Fox-Dobbs, K., Koch, P. L., Wayne, R. K., & Van Valkenburgh, B. (2007). Megafaunal Extinctions and the Disappearance of a Specialized Wolf Ecomorph. *Current Biology*, *17*(13), 1146–1150. https://doi.org/10.1016/j.cub.2007.05.072

Lerp, H., Wronski, T., Pfenninger, M., & Plath, M. (2011). A phylogeographic framework for the conservation of Saharan and Arabian Dorcas gazelles (Artiodactyla: Bovidae). *Organisms Diversity and Evolution*, *11*(4), 317–329. https://doi.org/10.1007/s13127-011-0057-z

Lézine, A. M., Hély, C., Grenier, C., Braconnot, P., & Krinner, G. (2011). Sahara and Sahel vulnerability to climate changes, lessons from Holocene hydrological data. *Quaternary Science Reviews*, *30*(21–22), 3001–3012. https://doi.org/10.1016/j.quascirev.2011.07.006

Li, H. (2011). A statistical framework for SNP calling, mutation discovery, association mapping and population genetical parameter estimation from sequencing data. *Bioinformatics*, *27*(21), 2987–2993. https://doi.org/10.1093/bioinformatics/btr509

Li, H., & Durbin, R. (2010). Fast and accurate long-read alignment with Burrows-Wheeler transform. *Bioinformatics*, *26*(5), 589–595. https://doi.org/10.1093/bioinformatics/btp698

Li, H., & Durbin, R. (2011). Inference of human population history from individual whole-genome sequences. *Nature*, *475*(7357), 493–496. https://doi.org/10.1038/nature10231

Li, H., Handsaker, B., Wysoker, A., Fennell, T., Ruan, J., Homer, N., … Durbin, R. (2009). The Sequence Alignment/Map format and SAMtools. *Bioinformatics*, *25*(16), 2078–2079. https://doi.org/10.1093/bioinformatics/btp352

Lindblad-Toh, K., Wade, C. M., Mikkelsen, T. S., Karlsson, E. K., Jaffe, D. B., Kamal, M., … Lander, E. S. (2005). Genome sequence, comparative analysis and haplotype structure of the domestic dog. *Nature*, *438*(7069), 803–819. https://doi.org/10.1038/nature04338

Linstädter, J., & Kröpelin, S. (2004). Wadi Bakht revisited: Holocene climate change and prehistoric occupation in the Gilf Kebir Region of the eastern Sahara, SW Egypt. *Geoarchaeology*, *19*(8), 753–778. https://doi.org/10.1002/gea.20023

Liu, Y. H., Wang, L., Xu, T., Guo, X., Li, Y., Yin, T. T., … Zhang, Y. P. (2018). Whole-Genome sequencing of African dogs provides insights into adaptations against tropical parasites. *Molecular Biology and Evolution*, *35*(2), 287–298. https://doi.org/10.1093/molbev/msx258

Lohmueller, K. E., Bustamante, C. D., & Clark, A. G. (2010). The effect of recent admixture on inference of ancient human population history. *Genetics*, *185*(2), 611–622. https://doi.org/10.1534/genetics.109.113761

Lorenzen, E. D., Heller, R., & Siegismund, H. R. (2012). Comparative phylogeography of African savannah ungulates. *Molecular Ecology*, *21*(15), 3656–3670. https://doi.org/10.1111/j.1365-294X.2012.05650.x

Martin, M. (2011). Cutadapt removes adapter sequences from high-throughput sequencing reads. *EMBnet.Journal*, *17*, 10–12.

McClymont, E. L., Sosdian, S. M., Rosell-Melé, A., & Rosenthal, Y. (2013). Pleistocene sea-surface temperature evolution: Early cooling, delayed glacial intensification, and implications for the mid-Pleistocene climate transition. *Earth-Science Reviews*, *123*, 173–193. https://doi.org/10.1016/j.earscirev.2013.04.006

McKenna, A., Hanna, M., Banks, E., Sivachenko, A., Cibulskis, K., Kernytsky, A., … DePristo, M. (2010). The Genome Analysis Toolkit: A MapReduce framework for analyzing next-generation DNA sequencing data. *Proceedings of the International Conference on Intellectual Capital, Knowledge Management & Organizational Learning*, *20*, 254–260. https://doi.org/10.1101/gr.107524.110.20

McQuillan, R., Leutenegger, A. L., Abdel-Rahman, R., Franklin, C. S., Pericic, M., Barac-Lauc, L., … Wilson, J. F. (2008). Runs of Homozygosity in European Populations. *American Journal of Human Genetics*, *83*(3), 359–372. https://doi.org/10.1016/j.ajhg.2008.08.007

McShane, T. O., & Grettenberger, J. F. (1984). Food of the golden jackal (Canis aureus) in central Niger. *African Journal of Ecology*, *22*(1), 49–53. https://doi.org/10.1111/j.1365-2028.1984.tb00673.x

Moehlman, P. D. (1986). Ecological Aspects of Social Evolution. *Ecological Aspects of Social Evolution*. https://doi.org/10.2307/j.ctt7zvwgq

Moodley, Y., & Bruford, M. W. (2007). Molecular biogeography: Towards an integrated framework for conserving Pan-African biodiversity. *PLoS ONE*, *2*(5). https://doi.org/10.1371/journal.pone.0000454

Moutinho, A. F., Serén, N., Paupério, J., Silva, T. L., Martínez-Freiriá, F., Sotelo, G., … Boratyński, Z. (2020). Evolutionary history of two cryptic species of northern African jerboas. *BMC Evolutionary Biology*, *20*(1), 1–16. https://doi.org/10.1186/s12862-020-1592-z

Muwanika, V. B., Nyakaana, S., Siegismund, H. R., & Arctander, P. (2003). Phylogeography and population structure of the common warthog (Phacochoerus africanus) inferred from variation in mitochondrial DNA sequences and microsatellite loci. *Heredity*, *91*(4), 361–372. https://doi.org/10.1038/sj.hdy.6800341

Nadachowska-Brzyska, K., Burri, R., Olason, P. I., Kawakami, T., Smeds, L., & Ellegren, H. (2013). Demographic Divergence History of Pied Flycatcher and Collared Flycatcher Inferred from Whole-Genome Re-sequencing Data. *PLoS Genetics*, *9*(11). https://doi.org/10.1371/journal.pgen.1003942

Nadachowska-Brzyska, K., Burri, R., Smeds, L., & Ellegren, H. (2016). PSMC analysis of effective population sizes in molecular ecology and its application to black-and-white Ficedula flycatchers. *Molecular Ecology*, *25*(5), 1058–1072. https://doi.org/10.1111/mec.13540

Nielsen, R., Mountain, J.L., Huelsenbeck, J.P., Slatkin, M. (1998). Maximum-Likelihood estimation of population divergence times and population phylogeny in models without mutation. *Evolution,* 52(3). 1998. pp. 669-677

Neukom, R., Steiger, N., Gómez-Navarro, J. J., Wang, J., & Werner, J. P. (2019). No evidence for globally coherent warm and cold periods over the preindustrial Common Era. In *Nature* (Vol. 571). https://doi.org/10.1038/s41586-019-1401-2

Ndiaye, A., Bâ, K., Aniskin, V., Benazzou, T., Chevret, P., Konečný, A., Sembène, M., Tatard, C., Kergoat, G.J. & Granjon, L. (2011). Evolutionary systematics and biogeography of endemic gerbils (Rodentia, Muridae) from Morocco: an integrative approach. —*Zoologica Scripta*, *41*, 11–28.

Nicholson, S. E., & Flohn, H. (1981). African climatic changes in late Pleistocene and Holocene and the general atmospheric circulation. *Sea Level, Ice and Climatic Change. Proc. Canberra Symposium, December 1979*, *2*, 295–301.

Nicolas, V., Bryja, J., Akpatou, B., Konecny, A., Lecompte, E., Colyn, M., Lalis, A., Couloux, C., Denys, C., & Granjon, L. (2008) . Comparative phylogeography of two sibling species of forest-dwelling rodent (*Praomys rostratus* and *P. tullbergi*) in West Africa: different reactions to past forest fragmentation. *Mol. Ecol.* 17, 5118–5134. doi: 10.1111/j.1365-294X.2008.03974.x

Nicolas, V., Granjon, L., Duplantier, J. M., Cruaud, C., & Dobigny, G. (2009). Phylogeography of spiny mice (genus Acomys, Rodentia: Muridae) from the south-western margin of the sahara with taxonomic implications. *Biological Journal of the Linnean Society*, *98*(1), 29–46. https://doi.org/10.1111/j.1095-8312.2009.01273.x

Nielsen, R., Korneliussen, T., Albrechtsen, A., Li, Y., & Wang, J. (2012). SNP calling, genotype calling, and sample allele frequency estimation from new-generation sequencing data. *PLoS ONE*, *7*(7). https://doi.org/10.1371/journal.pone.0037558

North Greenland Ice Core Project members (2004). High-resolution record of Northern Hemisphere climate extending into the last interglacial period. *Nature, 431*, 147–151.

Oetjens, M.T., Martin, A., Veeramah, K., & Kidd, J. (2018). Analysis of the canid Y-chromosome phylogeny using short-read sequencing data reveals the presence of distinct haplogroups among Neolithic European dogs. *BMC Genomics*, *19*: 350. https://doi.org/10.1186/s12864-018-4749-z

Pilot, M., Jedrzejewski, W., Branicki, W., Sidorovich, V. E., Jedrzejewska, B., Stachura, K., & Funk, S. M. (2006). Ecological factors influence population genetic structure of European grey wolves. *Molecular Ecology*, *15*(14), 4533–4553. https://doi.org/10.1111/j.1365-294X.2006.03110.x

Pilot, M., Moura, A. E., Okhlopkov, I. M., Mamaev, N. V., Alagaili, A. N., Mohammed, O. B., … Bogdanowicz, W. (2019). Global Phylogeographic and Admixture Patterns in Grey Wolves and Genetic Legacy of An Ancient Siberian Lineage. *Scientific Reports*, *9*(1), 1–13. https://doi.org/10.1038/s41598-019-53492-9

Purcell, S., Neale, B., Todd-Brown, K., Thomas, L., Ferreira, M. A. R., Bender, D., … Sham, P. C. (2007). PLINK: A tool set for whole-genome association and population-based linkage analyses. *American Journal of Human Genetics*, *81*(3), 559–575. https://doi.org/10.1086/519795

Rato, C., Brito, J. C., Carretero, M. A., Larbes, S., Shacham, B., & Harris, D. J. (2007). Phylogeography and genetic diversity of Psammophis schokari (Serpentes) in North Africa based on mitochondrial DNA sequences . *African Zoology*, *42*(1), 112–117. https://doi.org/10.1080/15627020.2007.11407383

Renaud, G., Hanghøj, K., Korneliussen, T. S., Willerslev, E., & Orlando, L. (2019). Joint Estimates of Heterozygosity and Runs of Homozygosity for Modern and Ancient Samples. *Genetics*, *212*(July), 587–614. https://doi.org/10.1534/genetics.119.302057

Rohling, E. J., Mayewski, P. A., & Challenor, P. (2003). On the timing and mechanism of millennial-scale climate variability during the last glacial cycle. *Climate Dynamics*, *20*(2–3), 257–267. https://doi.org/10.1007/s00382-002-0266-4

Rueness, E. K., Asmyhr, M. G., Sillero-Zubiri, C., Macdonald, D. W., Bekele, A., Atickem, A., & Stenseth, N. C. (2011). The cryptic African wolf: Canis aureus lupaster is not a golden jackal and is not endemic to Egypt. *PLoS ONE*, *6*(1). https://doi.org/10.1371/journal.pone.0016385

Sams, A. J., & Boyko, A. R. (2019). Fine-scale resolution of runs of homozygosity reveal patterns of inbreeding and substantial overlap with recessive disease genotypes in domestic dogs. *G3: Genes, Genomes, Genetics*, *9*(1), 117–123. https://doi.org/10.1534/g3.118.200836

Sereno, P. C., Garcea, E. A. A., Jousse, H., Stojanowski, C. M., Saliege, J. F., Maga, A., … Stivers, J. P. (2008). Lakeside cemeteries in the Sahara: 5000 years of holocene population and environmental change. *PLoS ONE*, *3*(8). https://doi.org/10.1371/journal.pone.0002995

Shchur, V. (2019). *MiSTI: PSMC-based Migration and Split Time Inference from two genomes*. https://github.com/vlshchur/MiSTI

Shchur, V., Korneliussen, T. S., & Nielsen, R. (2017). ngsPSMC: genotype likelihood-based PSMC for analysis of low coverage NGS. Retrieved from https://github.com/ANGSD/ngsPSMC

Simeneh, G. (2010). *Habitat use and Diet of Golden Jackal (Canis aureus) and Human-Carnivore Conflict in Guassa Community Conservation Area, Menz*. (MSc thesis) Addis Ababa University, Department of Biology.

Skoglund P, Ersmark E, Palkopoulou E, Dalen L. 2015. Ancient wolf genomereveals an early divergence of domestic dog ancestors and admixture into high-latitude breeds. *Curr Biol.* 25(11):1515–1519.

Skotte, L., & Albrechtsen, A. (2013). Estimating Individual Admixture Proportions from. *Genetics*, *195*(November), 693–702. https://doi.org/10.1534/genetics.113.154138

Skov, L., Macià, M. C., Sveinbjörnsson, G., Mafessoni, F., Lucotte, E. A., Einarsdóttir, M. S., … Stefansson, K. (2020). *The nature of Neanderthal introgression revealed by 27 , 566 Icelandic genomes*. (July 2019). https://doi.org/10.1038/s41586-020-2225-9

Smith, J. R. (2012). Spatial and temporal variations in the nature of Pleistocene pluvial phase environments across Africa. In *Modern Origins A North African perspective* (pp. 35–77).

Smitz, N., Berthouly, C., Cornélis, D., Heller, R., Van Hooft, P., Chardonnet, P., … Michaux, J. (2013). Pan-African Genetic Structure in the African Buffalo (Syncerus caffer): Investigating Intraspecific Divergence. *PLoS ONE*, *8*(2), 1'17.

Sommer, R. S., & Nadachowski, A. (2006). Glacial refugia of mammals in Europe: Evidence from fossil records. *Mammal Review*, *36*(4), 251–265. https://doi.org/10.1111/j.1365-2907.2006.00093.x

Stöck, M., Dufresnes, C., Litvinchuk, S. N., Lymberakis, P., Biollay, S., Berroneau, M., … Perrin, N. (2012). Cryptic diversity among Western Palearctic tree frogs: Postglacial range expansion, range limits, and secondary contacts of three European tree frog lineages (Hyla arborea group). *Molecular Phylogenetics and Evolution*, *65*(1), 1–9. https://doi.org/10.1016/j.ympev.2012.05.014

Tajima, F. (1989). Statistical method for testing the neutral mutation hypothesis by DNA polymorphism. *Genetics*, *123*(3), 585–595. https://doi.org/PMC1203831

Tamar, K., Metallinou, M., Wilms, T., Schmitz, A., Crochet, P. A., Geniez, P., & Carranza, S. (2018). Evolutionary history of spiny-tailed lizards (Agamidae: Uromastyx) from the Saharo-Arabian region. *Zoologica Scripta*, *47*(2), 159–173. https://doi.org/10.1111/zsc.12266

Tange, O. (2018). *GNU Parallel 2018*. https://doi.org/10.5281/zenodo.1146014

Team, R. C. (2017). *R: A language and environment for Statistical computing. R Foundation for Statistical Computing, Vienna, Austria.* URL: https://www.R-project.org/.

Temu, S. E., Nahonyo, C. L., & Moehlman, P. D. (2016). *Comparative Foraging Efficiency of Two Sympatric Jackals , Silver-Backed Jackals (Canis mesomelas) and Golden Jackals (Canis aureus), in the Ngorongoro Crater , Tanzania*. *2016*. https://doi.org/10.1155/2016/6178940

Temu, S. E., Nahonyo, C. L., & Moehlman, P. D. (2018). Diet composition of the golden jackal (Canis aureus) in the Ngorongoro Crater, Tanzania. *Tanzania Journal of Science*, *44*(1), 52-61–61.

Tison, J. L., Edmark, V. N., Sandoval-Castellanos, E., Van Dyck, H., Tammaru, T., Välimäki, P., … Gotthard, K. (2014). Signature of post-glacial expansion and genetic structure at the northern range limit of the speckled wood butterfly. *Biological Journal of the Linnean Society*, *113*(1), 136–148. https://doi.org/10.1111/bij.12327

Tjallingii, R. I. K., Claussen, M., Stuut, J. W., Fohlmeister, J., Jahn, A., Bickert, T., … Ohl, U. R. (2008). Coherent high- and low-latitude control of the northwest African hydrological balance. *Nature Geoscience*, *1*, 670–675. https://doi.org/10.1038/ngeo289

Trauth, M. H., Larrasoaña, J. C., & Mudelsee, M. (2009). Trends, rhythms and events in Plio-Pleistocene African climate. *Quaternary Science Reviews*, *28*(5–6), 399–411. https://doi.org/10.1016/j.quascirev.2008.11.003

Urios, V., Donat-Torres, M. P., Monroy-Vilchis, C. R. O., & Idrissi, H. R. (2015). El análisis del genoma mitocondrial del cánido estudiado en Marruecos manifiesta que no es ni lobo (Canis lupus) ni chacal euroasiático (Canis aureus). *Altotero*, *3*.

Van Valkenburgh, B., & Wayne, R. K. (1994). Shape Divergence Associated with Size Convergence in Sympatric East African Jackals. *Ecology*, *75*(6), 1567–1581.

Vieira, F. G., Fumagalli, M., Albrechtsen, A., & Nielsen, R. (2013). Estimating inbreeding coefficients from NGS data: Impact on genotype calling and allele frequency estimation. *Genome Research*, *23*(11), 1852–1861. https://doi.org/10.1101/gr.157388.113

1078 Waters, S., Harrad, A. El, Amhaouch, Z., Taiqui, L., & Senn, H. (2015). Distribution update DNA analysis
1079 confirms African wolf in Morocco. *Canid Biology & Conservation*, *18*(5), 15–17.
1080 https://doi.org/10.1371/journal.pone.0016385.

1081 Watterson, G. (1975). On the number of segregating sites in genetical models without recombination.
1082 *Theoretical Population Biology*, *7*, 256–276.

1083 Weldeab, S., Lea, D. W., Schneider, R. R., & Andersen, N. (2007). 155,000 Years of West African
1084 Monsoon and Ocean Thermal Evolution. *Science*, *316*, 1303–1307.
1085 https://doi.org/10.1126/science.1140461

1086 Werdelin, L., & Lewis, M. E. (2005) Plio-Pleistocene Carnivora of eastern Africa: species richness and
1087 turnover patterns. *Zoological Journal of the Linnean Society,* 144(2), 121–144,
1088 https://doi.org/10.1111/j.1096-3642.2005.00165.x

1089 Yeakel, J. D., Pires, M. M., Rudolf, L., Dominy, N. J., Koch, P. L., Guimarães, P. R., & Gross, T. (2014).
1090 Collapse of an ecological network in Ancient Egypt. *Proceedings of the National Academy of*
1091 *Sciences of the United States of America*, *111*(40), 14472–14477.
1092 https://doi.org/10.1073/pnas.1408471111

1093 Zeng, K., Fu, Y. X., Shi, S., & Wu, C. I. (2006). Statistical tests for detecting positive selection by utilizing
1094 high-frequency variants. *Genetics*, *174*(3), 1431–1439. https://doi.org/10.1534/genetics.106.061432
1095

Figure captions

Figure 1. Map of Africa showing isohyets, elevations, main water sources, African golden wolf distribution (in green) according to IUCN and location of the seven samples included in this study (in red).

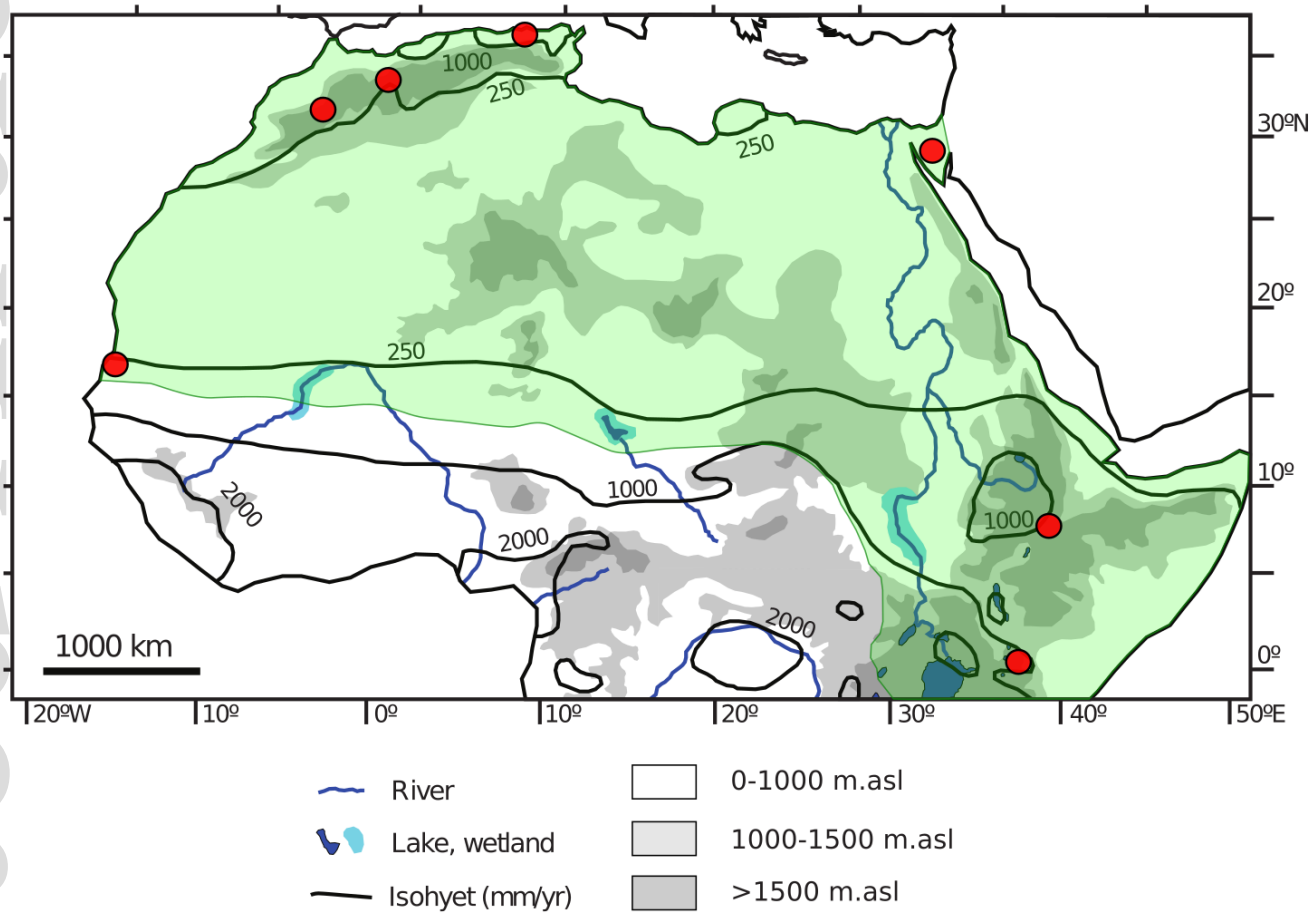

Figure 2. NGSadmix plots of Old World canids showing admixture proportions, including the 23 individuals used at this study mapped against African hunting dog (A) and only African golden wolves (B). Eastern (Kenya, Ethiopia) African golden wolves cluster in a different group from those from the north (Egypt, Algeria, east Morocco, west Morocco, Senegal). The Egyptian individual also seems to have ancestry from gray wolves or domestic dogs. EW: Ethiopian wolf. EGJ: Eurasian golden jackal. Plots are based in 9.885M sites (see text for details).

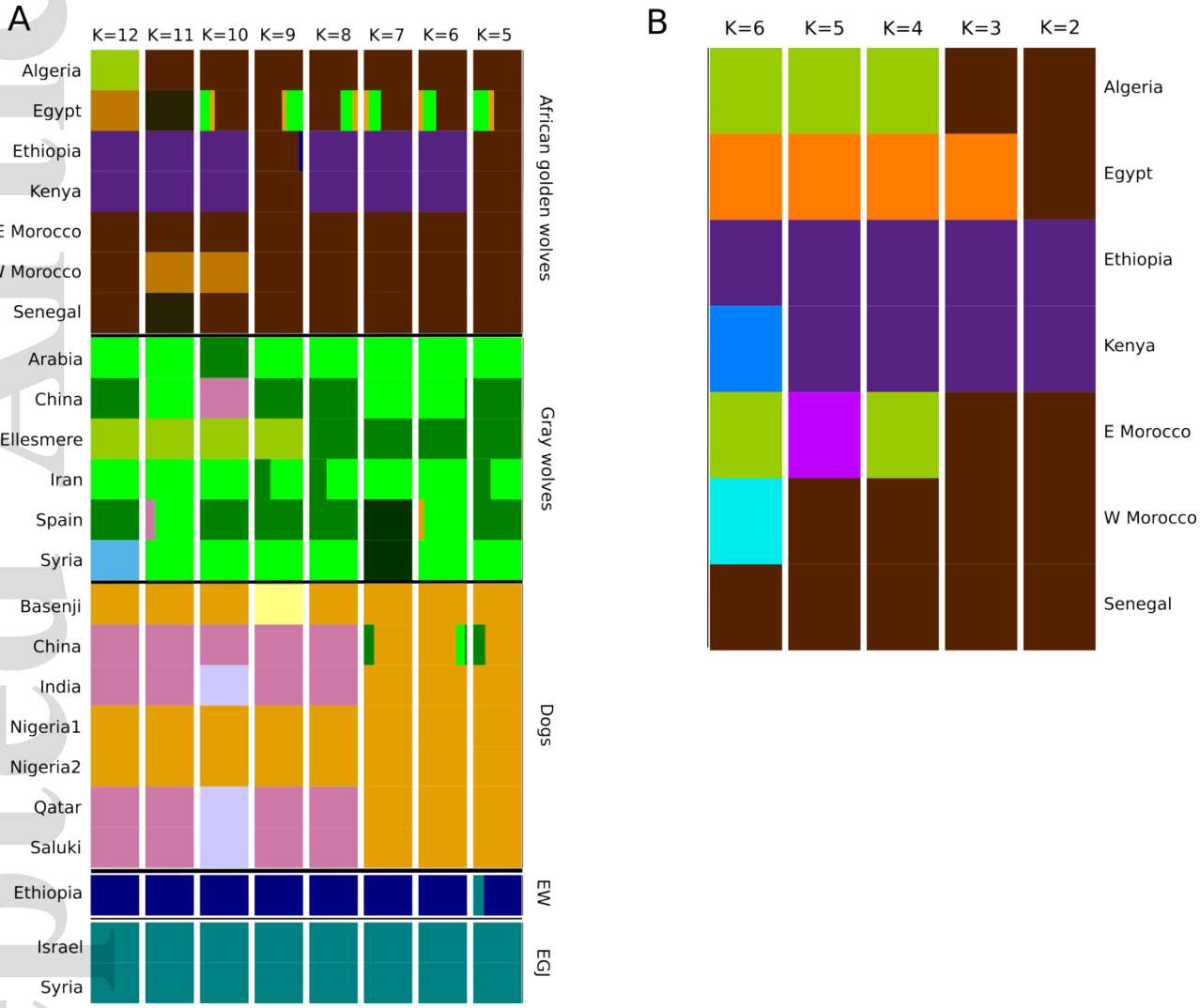

Figure 3. PSMC plot of six African golden wolf individuals: Algeria, west Morocco, east Morocco, Senegal, Ethiopia, Kenya. Consensus sequences were extracted from .bam files and Θ_0 values were corrected according to the False Negative Rate (FNR) calculated for each actual coverage by down sampling the Kenyan genome (24X). Individual PSMC plots were bootstrapped 50 times each. Proposed Green Sahara Periods (GSPs) were included from Larrasoaña et al., (2013) and Ehrmann et al., (2017). Heinrich events (H) of local cooling were also included according to Rohling et al. (2003) and Ehrmann et al. (2017). The black line defines the event of speciation (ca. 1.3 Myr ago) according to Koepfli et al. (2015) and Chavez et al. (2019) and a confidence interval of 1.10-1.5 Myr (Chavez et al., 2019). Numbers after each individual mean FNR calculated by visually adjusting using the psmc_plot.py program from the PSMC package.

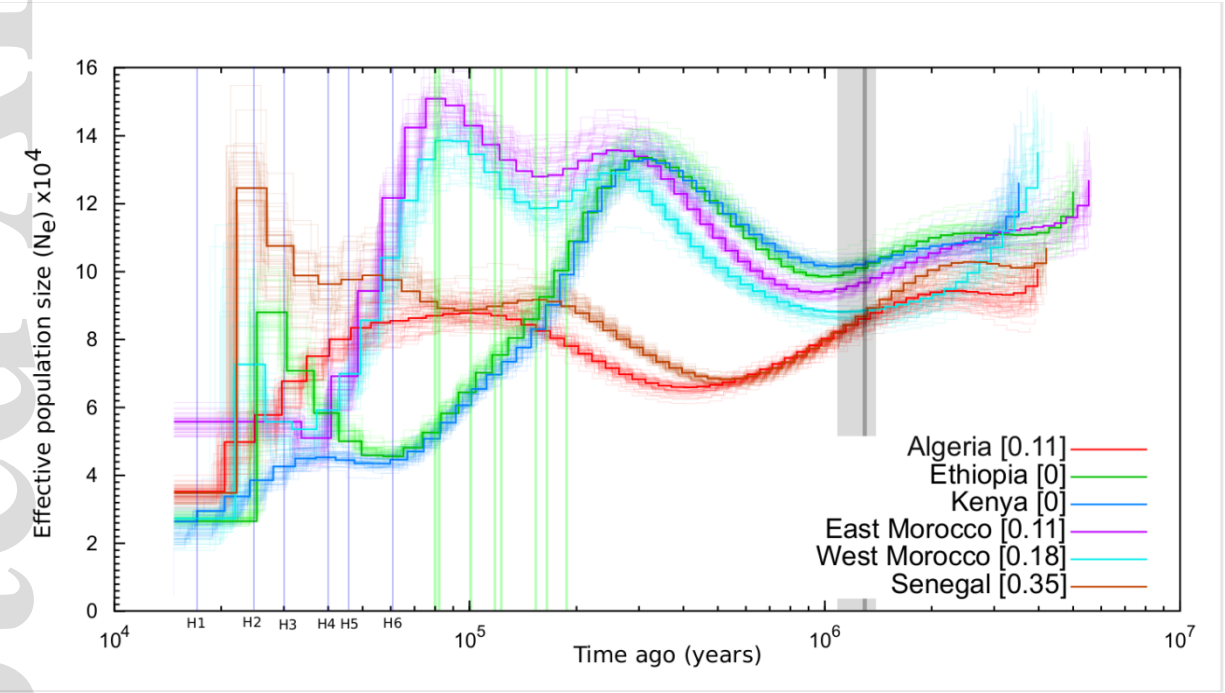

Figure 4. ngsPSMC plots of the seven African golden wolf individuals of this study. (A) ngsPSMC plot of all individuals using maximum Ne =17000. (B) ngsPSMC plot using maximum Ne = 2000. Cooling events (H) are the same as in **Figure 3**. Local events of wetter conditions are marked up (north Sahara: 65-61 ka, 52.5-50.5 ka and 37.5-33 ka (Hoffmann et al., 2016)) and down (Sahel: 55-60 ka; (Tjallingi et al., 2008; Weldeab et al., 2007)) of Figure 4A**.** HO = Holocene Optimum as in Larrasoaña et al., (2013). YD = Younger Dryas.

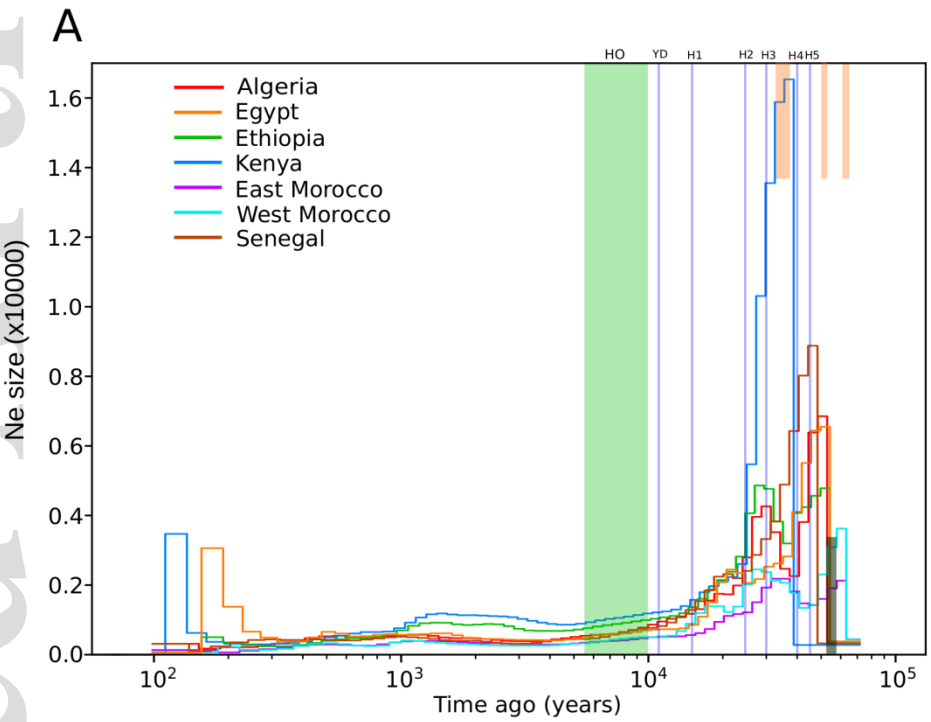

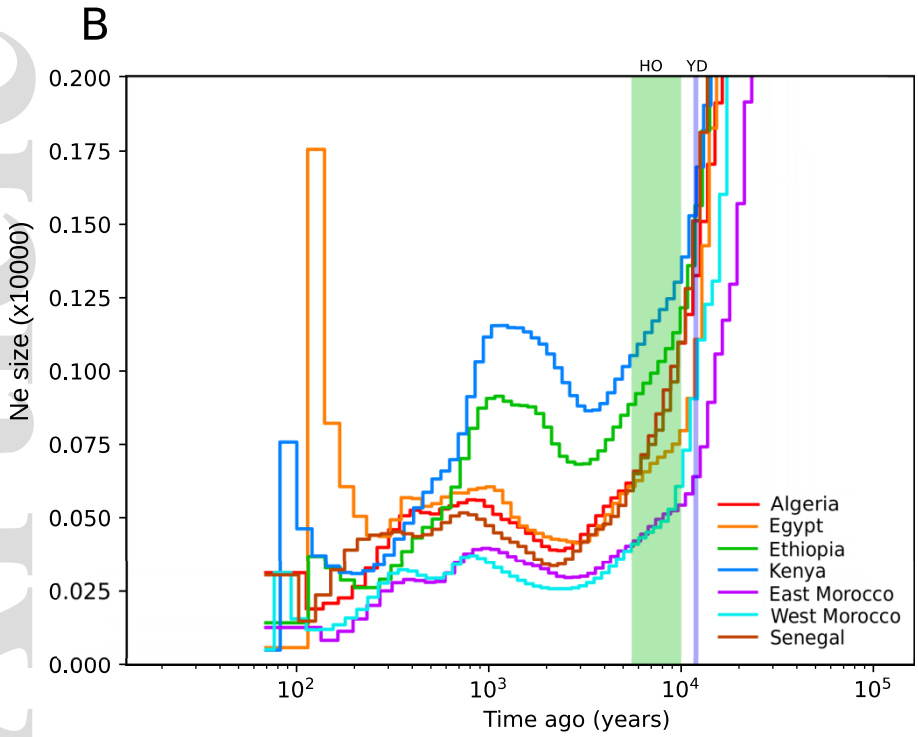

1129
1130
1131
1132

Figure 5. Times of divergence between pairs of lineages of African golden wolves. $\delta^{18}O$ data from the North Greenland Ice Core Project (NGRIP members, 2004) are shown, along with main glacial and interglacials periods, for the last 125,000 years. Intervals for divergence of pairs of lineages were considering the top 5% (light gray) and 1% (dark gray) of values for polynomial equations of adjusted graphs to the data points after R^2=0.99. For further explanation, see **Table S8**. H bars: Heinrich events. YD: Younger Dryas.

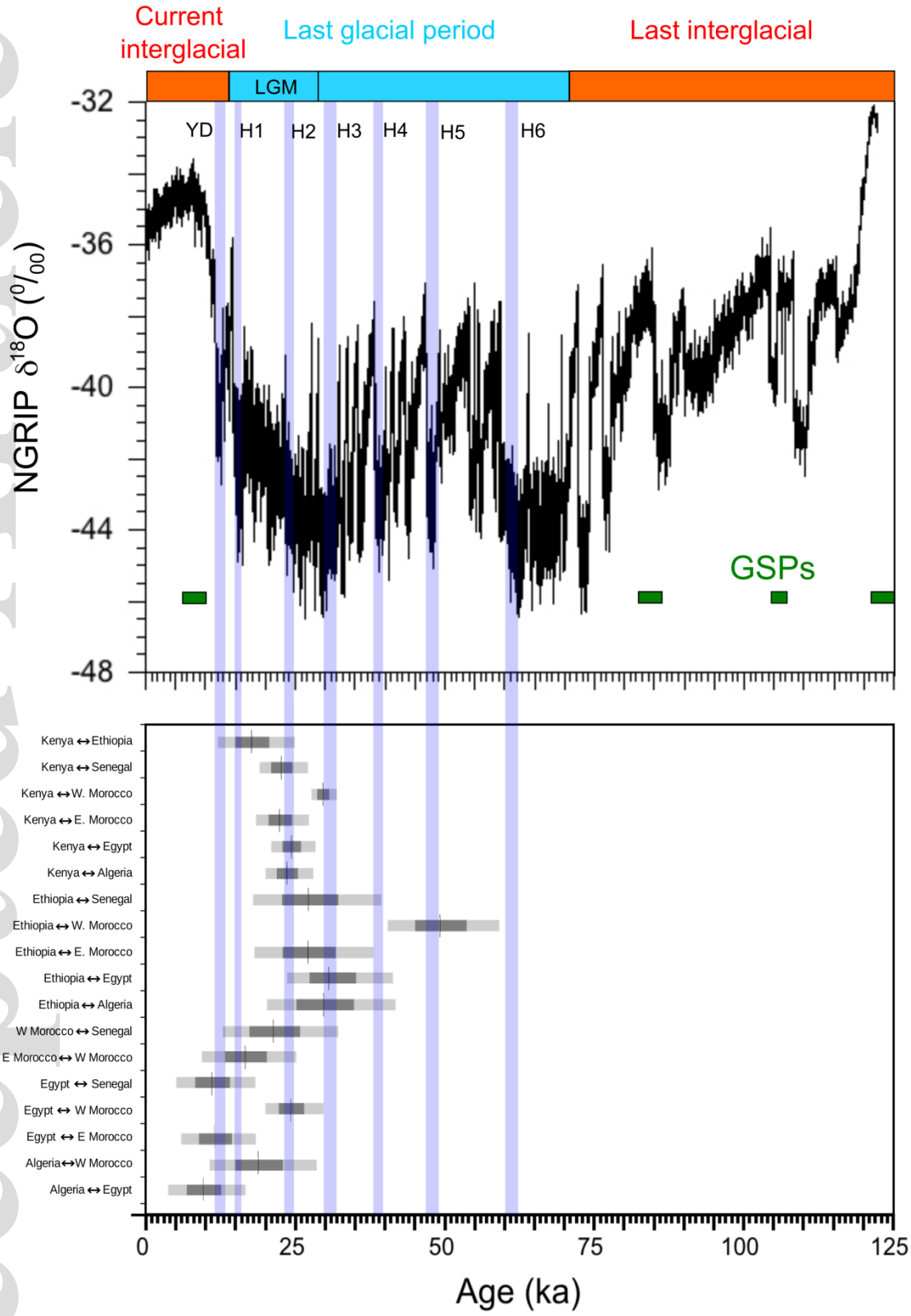

Figure 6. Dust flux record of Ocean Drilling Program (ODP) Leg 160, site 967 (Larrasoaña et al., 2003) of eastern Mediterranean Sea from last three million years (Ma). We have incorporated an estimation of the onset

1142 of the mid-Pleistocene climate Transition (MPT) (McClymont et al., 2013), the shift from 41-kyr- to 100-kyr-
1143 long aridity cycles and a represents a breakpoint in north African aridity (Trauth et al., 2009). Estimation of the
1144 speciation event of African golden wolves circa 1.32 million years ago (Ma) is also included with confidence
1145 intervals (blue: 1.0-1.65, Koepfli et al. (2015); red: 1.1-1.5, Chavez et al. (2019)).
1146

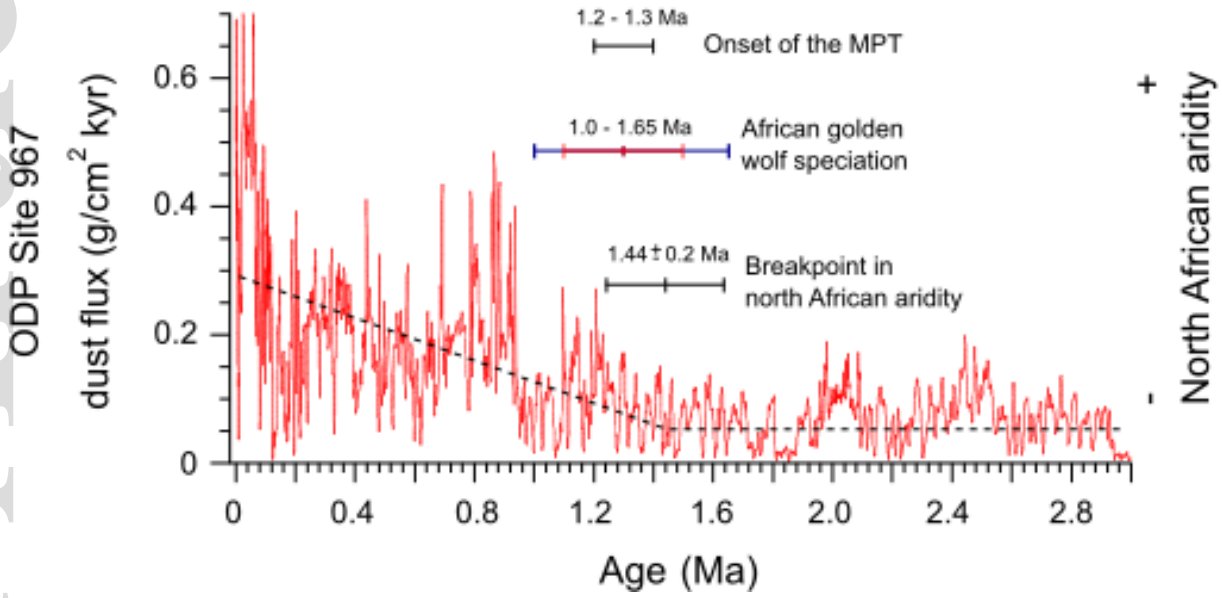

1147

Supplementary figure captions

Supplementary Figure 1. PSMC plots of African golden wolf (AGW) genomes under different conditions. A, B represent PSMC plots of the Kenyan AGW with the normal (24X) and downsampled coverages (15X, 11.2X, 9X, 7X) without (A) and with (B) False Negative Rate correction for low heterozygosity due to low coverages. C, D represent PSMC plots of six AGW (Algeria, Ethiopia, Kenya, East Morocco, West Morocco, Senegal) with lower (C) and upper (D) bounds of the mutation rate estimation by Koch et al., (2019) (2.7-7.1*10^{-9}).

Supplementary Figure 2. Genotype likelihood-based Principal Component Analysis (PCA) generated by ngsCovar from the ngsTools package. PCA was called using 2.54 million sites in 16 genomes of wild Old World canids (African golden wolves, gray wolves, Ethiopian wolves, Eurasian golden jackals) and 7 genomes of domestic dogs.

Supplementary Figure 3. SNP-based Principal Component Analysis (PCA) of 23 canid individuals. SNPs were called based in genotype likelihood using ANGSD with the -doPlink option, curated and filtered for Hardy-Weinberg equilibrium and linkage disequilibrium using PLINK v1.9. PCA was generated by flashPCA using 625,000 sites in 16 genomes of wild Old World canids (African golden wolves, gray wolves, Ethiopian wolves, Eurasian golden jackals) and 7 genomes of domestic dogs.

Supplementary Figure 4. Best-fit calculation of K (likelihood) vs values of K as calculated by NGSadmix using 23 genomes of Old World canids mapped against African hunting dog (admixture plot in **Figure 2**).

Supplementary Figure 5. SNP-based Admixture plots of Old World canids mapped against African hunting dog showing admixture proportions, including the 23 individuals used at this study. SNPs were called as in **Supplementary Figure 2**. Eastern (Kenya, Ethiopia) African golden wolves cluster in a different group from those from the north (Egypt, Algeria, East Morocco, West Morocco, Senegal). EW: Ethiopian wolf. EGJ: Eurasian golden jackal. This plot is based in 625,000 unlinked sites.

Supplementary Figure 6. Thetas per site and neutrality tests of four populations: east African Golden Wolves (AGW) (Ethiopia, Kenya), northwest AGW (Algeria, east Morocco, west Morocco, Senegal), Coyote (California, Midwest, Mexico), Gray wolves of the Middle East (ME) (S. Arabia, Iran, Syria). We considered 50-kb non-overlapping windows across the whole genome and filtered out those windows with a number of

sites outside the 99.7% of the distribution (mean +/- 3 standard deviations). Theta statistics were calculated dividing by the total number of sites. Neutrality tests were averaged per window.

Supplementary Figure 7. Genome wide heterozygosity calculated per individual and population. Heterozygosity was calculated using the fraction of singletons from the unfolded Site-Frequency Spectrum (SFS). Genome wide heterozygosities were corrected using the Kenyan African golden wolf genome (24X) and down sampling it to each coverage, calculating proportion of lost heterozygosity for each coverage. Corrections are marked in darker colors. AGW: African golden wolves. GW: gray wolves. EGJ: Eurasian golden jackals.

Supplementary Figure 8. Heterozygosity plots of east and west Moroccan individuals per chromosome. Plots were generated with ROHan using 500kB windows, minimum coverage of 5X and maximum coverage of 2.5 times the mean coverage per genome. --rohmu option were set as 2e-5. All other settings were left as default.

Supplementary Figure 9. Log-likelihood of divergence between members of the north African golden wolf cluster (A) and north vs. east African golden wolf cluster (B) vs time. Likelihood of divergence times was calculated paralellizing MiSTI with GNU Parallel using the default optimization round. Time segments were defined using likely aridization / regreening Sahara periods defined in the literature. A polynomial curve equation was adjusted to the fifth degree and plotted when $R^2 > 0.99$.

Table 1. Mean values and standard deviations of genome wide thetas per site and neutrality tests of four populations: northwest African Golden Wolves (AGW) (Algeria, east Morocco, west Morocco, Senegal), east AGW (Ethiopia, Kenya), gray wolves of the Middle East (ME) (S. Arabia, Iran, Syria), and coyote (California, Midwest, Mexico). We considered 50-kb non-overlapping windows across the whole genome and filtered out those windows with a number of sites outside the 99.7% of the distribution (mean +/- 3 standard deviations). Theta statistics were calculated dividing by the total number of sites. Neutrality tests were averaged per window. Θ_W: Watterson's theta (Watterson, 1975). $\Theta\pi$: Nucleotide diversity (Tajima, 1989). Θ_{FL}: Fu and Li's theta (Fu & Li, 1993). Θ_H: Fay and Wu's theta (Fay & Wu, 2000). Θ_L: Fu and Li's L (Fu & Li, 1993). Neutrality tests: Tajima's D (Tajima, 1989); Fu's F and D (Fu & Li, 1993); Fay's H (Fay et al., 2006); Zeng's E (Zeng et al., 2006).

	Thetas					Neutrality tests				
Populations	Θ_W	$\Theta\pi$	Θ_{FL}	Θ_H	Θ_L	Tajima's D	Fu's F	Fu's D	Fay's H	Zeng's E
northwest AGW	$8.52 \pm 3.96*10^{-4}$	$8.55 \pm 4.15*10^{-4}$	$4.62 \pm 2.35*10^{-4}$	$1.7 \pm 0.77*10^{-3}$	$1.28 \pm 0.59*10^{-3}$	$-0.34 \pm 3.98*10^{-1}$	$7.92 \pm 4.32*10^{-1}$	$9.06 \pm 3.63*10^{-1}$	-1.54 ± 0.41	$9.13 \pm 2.08*10^{-1}$
east AGW	$7.77 \pm 4.42*10^{-4}$	$7.93 \pm 4.53*10^{-4}$	$4.61 \pm 2.99*10^{-4}$	$1.17 \pm 0.64*10^{-3}$	$9.55 \pm 5.43*10^{-4}$	$2.09 \pm 6.12*10^{-1}$	1.04 ± 0.65	1.04 ± 0.55	-1.22 ± 0.58	$7.79 \pm 2.69*10^{-1}$
ME gray wolves	$8.47 \pm 4.06*10^{-4}$	$8.49 \pm 4.19*10^{-4}$	$4.87 \pm 2.53*10^{-4}$	$1.49 \pm 0.71*10^{-3}$	$1.17 \pm 0.56*10^{-3}$	$-0.19 \pm 4.02*10^{-1}$	$8.03 \pm 4.45*10^{-1}$	$8.87 \pm 3.77*10^{-1}$	-1.46 ± 0.44	$8.81 \pm 2.2*10^{-1}$
coyote	$7.61 \pm 3.88*10^{-4}$	$7.71 \pm 4.02*10^{-4}$	$4.24 \pm 2.48*10^{-4}$	$1.33 \pm 0.68*10^{-3}$	$1.05 \pm 0.54*10^{-3}$	$-0.19 \pm 4.02*10^{-1}$	$8.03 \pm 4.45*10^{-1}$	$8.87 \pm 3.77*10^{-1}$	-1.46 ± 0.44	$8.81 \pm 2.2*10^{-1}$

Table 2. Pairwise genome wide F_{ST} values of African golden wolves (A), gray wolves (B) and coyotes (C). F_{ST} values were calculated with the ngsTools package. Distances in km between coordinates were calculated in Marble (Linux).

A

African golden wolves								
	Algeria	Egypt	east Morocco	west Morocco	Senegal	Ethiopia	Kenya	
distances (km)		2.01×10^{-1}	6.09×10^{-2}	2.05×10^{-1}	9.5×10^{-2}	2.38×10^{-1}	4.05×10^{-1}	Algeria
	2590		1.67×10^{-1}	3.04×10^{-1}	2.09×10^{-1}	2.92×10^{-1}	4.4×10^{-1}	Egypt
	920	3400		1.7×10^{-1}	8.11×10^{-2}	2.15×10^{-1}	3.62×10^{-1}	east Morocco
	1300	3780	390		2.19×10^{-1}	3.46×10^{-1}	5.04×10^{-1}	west Morocco
	3250	5270	2420	2060		2.35×10^{-1}	4.04×10^{-1}	Senegal
	4610	2530	5170	5420	6110		2.89×10^{-1}	Ethiopia
	5170	3290	5630	5840	6220	850		Kenya

B

Gray wolves				
	S. Arabia	Iran	Syria	
distances (km)		1.73×10^{-1}	2.54×10^{-1}	S. Arabia
	1270		1.66×10^{-1}	Iran
	1390	1360		Syria

C

Coyotes				
	California	Mexico	Midwest	
distances (km)		1.62×10^{-1}	1.15×10^{-1}	California
	1060		1.34×10^{-1}	Mexico

	2770	2590		Midwest

1167

Table 3. Values of inbreeding coefficients (Fi) using genomewide genotype likelihood and SNP-based approaches (ngsF, PLINK and ROHan, respectively) and using the ROH-based method of McQuillan et al. (2008) with ROHs calculated with genotype likelihood and SNP-based approaches (ROHan and PLINK, respectively). Values higher than 0.1 are marked in gray.

		F_i (ngsF)	F_i (PLINK)	F_{ROH} (PLINK) 500kb	F_{ROH} (ROHan) min 500kb	F_{ROH} (ROHan) med 500kb	F_{ROH} (ROHan) max 500kb
AGW	Algeria	$1.17x10^{-2}$	$4.66x10^{-2}$	$2.34x10^{-7}$	0	0	$2.27x10^{-4}$
	Egypt	$1.35x10^{-1}$	$6.49x10^{-2}$	$8.46x10^{-6}$	0	0	0
	East Morocco	$5.88x10^{-4}$	0	0	0	0	$2.27x10^{-4}$
	West Morocco	$2.51x10^{-1}$	$2.93x10^{-1}$	$3.34x10^{-6}$	0	0	0
	Senegal	$2.65x10^{-2}$	$8.49x10^{-2}$	$7.17x10^{-7}$	0	0	$6.81x10^{-4}$
	Ethiopia	$2.20x10^{-5}$	0	$9.70x10^{-4}$	0	0	$2.27x10^{-4}$
	Kenya	$6.04x10^{-2}$	$1.47x10^{-1}$	$9.53x10^{-4}$	$1.16x10^{-2}$	$2.68x10^{-2}$	$2.68x10^{-2}$
GW	S. Arabia	$8.47x10^{-2}$	$1.81x10^{-1}$	$1.47x10^{-5}$	0	0	$4.54x10^{-4}$
	Iran	$1.90x10^{-5}$	0	$1.05x10^{-5}$	$4.76x10^{-3}$	$1.18x10^{-2}$	$1.66x10^{-2}$
	Syria	$7.21x10^{-2}$	$1.57x10^{-1}$	$1.77x10^{-5}$	0	0	$4.54x10^{-4}$
Coyotes	California	$9.60x10^{-5}$	0	$4.27x10^{-5}$	$1.86x10^{-2}$	$4.13x10^{-2}$	$4.70x10^{-2}$
	Mexico	$9.77x10^{-3}$	$5.70x10^{-2}$	$2.10x10^{-5}$	0	0	$8.17x10^{-3}$